

Acknowledgments

I would like to express my sincere thanks and deep gratitude to my supervisors Dr. Fatin Abdul Jalil Al-Moudarris for suggesting the present project, and Dr. Uday Ali Al-Obaidy for completing the present work and for their support and encouragement throughout the research.

I am most grateful to the Dean of College of Science and Head and the staff of the Department of Physics at Al-Nahrain University, particularly Ms. Basma Hussain for her assistance in preparing some of the diagrams.

The assistance given by the staff of the library of the College of Science at Baghdad University is highly appreciated.

Finally, I most grateful to my parents, my brothers, Laith, Hussain, Firas, Mohamed, Omer and my sisters, Sundus, Enas and Muna for their patience and encouragement throughout this work, and to my friends particularly Fatma Nafaa, Suheel Najem and Yousif Suheel, for their encouragement and to for their support.

Sura

Certification

We certify that this thesis entitled “**Determination of the Most Favorable Shapes for the Electrostatic Quadrupole Lens**” is prepared by **Sura Allawi Obaid Al-Zubaidy** under our supervision at the College of Science of Al-Nahrain University in partial fulfillment of the requirements for the degree of **Master of Science in Physics**.

Signature:

Name: Dr. Fatin A. J. Al-Moudarris

Title: (Supervisor)

Date: / 4 / 2007

Signature:

Name: Dr. Uday A. H. Al-Obaidy

Title: (Supervisor)

Date: / 4 / 2007

In view of the recommendations, we present this thesis for debate by the examination committee.

Signature:

Name: Dr. Ahmad K. Ahmad

(Assist. Prof.)

Head of Physics Department

Date: / 2 / 2007

1- INTRODUCTION

1-1 Electrostatic Quadrupole Lens

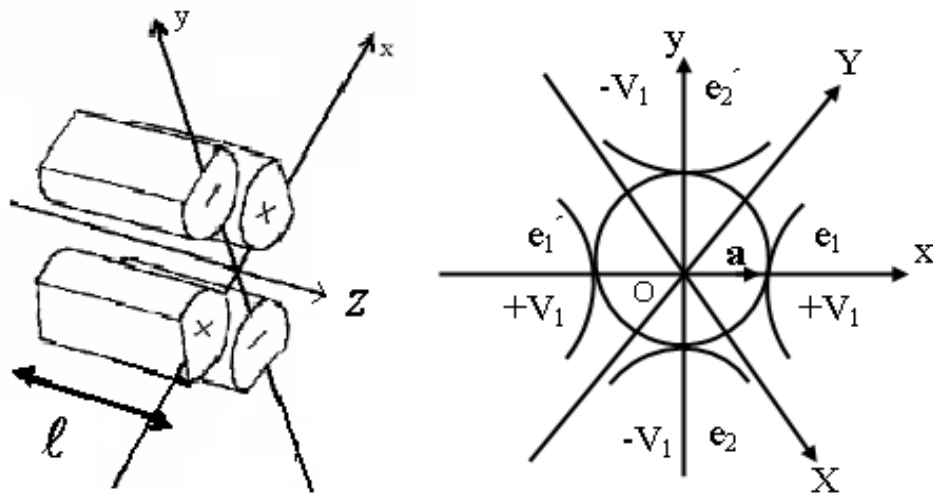
Electrostatic Quadrupole lens is not widely used in place of conventional round lenses because it is not easy to produce stigmatic and distortion-free images. The control of the quadrupole lens system is much complicated than in the case of round lenses because the combination of the quadrupole lenses has an extremely asymmetrical lens action [Okayama et al. 1978].

Electrostatic quadrupole lenses are important elements for focusing of accelerated charged particles. Their focusing action, however, is described only in Gaussian or first order approximation [Matsuda and Wollink 1972]. Electrostatic quadrupole lenses, although effective in focusing ions of high mass, have achromatic aberration coefficients which can be considerable [Martin 1991]. The most distinctive feature of electrostatic lens is that for non-relativistic case the focusing properties as well as the aberration are independent of the charge - to- mass quotient of the particles. Therefore, if a system is to be used with different ions, electrostatic lens must be applied. Furthermore, only potential ratio has influence on the lens properties. The only major manufacturing problems are electric breackdown and accumulation of charges on the insulating surfaces. Under vacuum pressure of about 10^{-6} torr the electrodes must be separated from each other so that the maximum field strength does not exceed 15 kV/mm [Szilagyi 1988].

Electrostatic quadrupole lenses are often preferable to magnetic ones for focusing beams of moderate energy. They are also preferable for dealing with ion beams since the focal length of an electrostatic lens does not depend on the charged particles mass as it does for a magnetic lens.

However, quadrupole lens systems are more sensitive to mechanical defects than round ones [Baranova and Read 2001].

An electrostatic quadrupole lens has a four-fold symmetry with respect to the optical axis. Its adjacent electrodes are at $\frac{\pi}{4}$ angle with each other. The detailed description of their potential arrangement is shown in figure (1-1), where e_1 and e_1° are at a potential $+V_1$ and the other pair of electrodes e_2 and e_2° are set at a potential $-V_1$. The planes that do not intersect the electrodes are defined by zOX and zOY and the other planes, which intersect the electrodes, are defined by zOx and zOy . The z -axis is normal to the plane of the paper at O . The aperture of the lens is defined by the radius a of a circular channel, which is tangential to the four electrodes [Hawkes 1970].



(a)

(b)

Figure (1-1): Electrostatic quadrupole lens, (a) The polarities of the electrodes of lens in the x and y axes (b) A transverse cross-section of an electrostatic quadrupole lens [Grivet 1972].

If a positively-charged particle is incident parallel to the axis in the plane zOx , it will experience a repulsion due to the electrode e_1 (or e_1^{\ominus}), but will not be affected by the presence of e_2 and e_2^{\ominus} as a result of the symmetry. The particle will remain in the plane zOx , and will converge toward the axis. In the plane zOy , the trajectory will also be planar, but the particle will be attracted by e_2 (or e_2^{\ominus}) and will diverge away from the axis. Particles, which are incident at the lens, other than in the planes zOx and zOy , will follow skew trajectories, approaching the optical axis Oz in the Ox direction, but moving away from Oz in the Oy direction. Therefore, in one direction there is the effect of convergence and in the other of divergence as shown in figure (1-2).

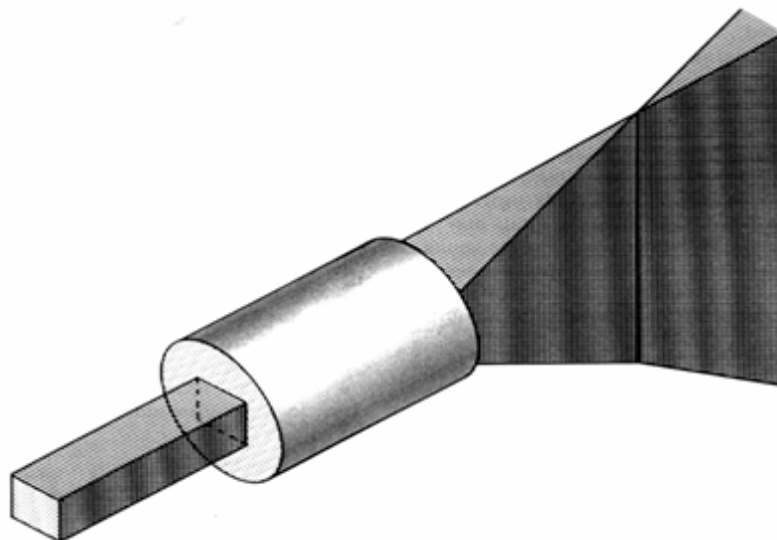


Figure (1-2): The action of a single quadrupole lens on a charged-particles beam; convergence in the horizontal plane and divergence in the vertical plane form a line image,[Grime and Watt1988].

Quadrupole lens is described as converging if particles moving in x-z plane are deflected toward the axis and diverging if particles moving in y-z plane are deflected away from the axis [Grime and Watt 1988].

The quadrupole lens is more complex than the axial symmetrical in construction, in calculations and in operation, and the focusing quadrupole systems usually do not produce a regular image of an object because in two mutually perpendicular planes xOz and yOz they have different positions of focal points, focal planes, and different magnifications and aberrations. At specific symmetry of the quadrupole system geometry, it is possible to obtain in both planes xOz and yOz the same positions of the focal points and the focal planes, the same magnifications and even the same spherical aberrations [Dymnikov et al. 2005].

The power of a quadrupole lens can be rised by increasing not only the field gradient but also the effective length of the lens field. Hence, there are no major restrictions on the beam energy. Since quadrupole can focus in only transverse direction [Abramovich et al. 2005].

1-2 Quadrupole Lenses Applications

Studies on quadrupole lenses concentrated on their application as corrector units for reducing the spherical aberration [Hawkes 1970]. Quadrupole lens are commonly used for focusing electron and ion beams of high energy. An example of such device is the ion implanter [Baranova and Read 1998].

Charge particle lenses are widely used in modern science. During the initial period of their development axial symmetrical lenses received intensive application in electron beam instruments. The transmission electron microscope (TEM) is similar to the biological light microscope to the extent that electrons pass through a thin specimen and are then imaged by appropriate lenses. The scanning electron microscope (SEM), proposed soon after the TEM, is smaller to a TEM but uses the same kind of electromagnetic lenses for focusing. In the SEM, focusing lenses do not produce an image of the specimen, but instead the electrons are focused into a very small spot (probe) which is then scanned across the surface of a specimen. The fine-probe scanning technique combined with the idea of forming the image from transmitted electrons resulting a scanning-transmission electron microscope (STEM) appeared [Dymnikov et al 2005].

A new ion optical element of mass spectrometry has been developed to increase ion beam transmission into the high vacuum region of mass spectrometry. A new mass spectrometry ion optical element, termed the electrostatic quadrupole extraction lens (EQEL), has been developed that incorporates quadrupole – like focusing fields in to an extraction lens. The EQEL optic was modeled using Simion 7 software and a range of optimum potentials was found for which high transmission occurred.

Such optics can be readily applied to other mass spectrometers, as most instruments already contain a similarly shaped extraction optics. This device should prove useful with ionization sources other than a glow discharge, though its effectiveness will be greatest when applied to instruments whose ion beam experiences minimal space - charge related divergence [Barnes et al 2003].

A quadrupole doublet is also employed in electron - optical devices of moderate accelerating voltage when astigmatic focusing is required. For example in electron and mass spectrometer containing sector magnets or electrostatic cylindrical analyzers which are themselves astigmatic, quadrupole lenses enable better beam matching than conventional axially symmetrical lenses. There are also some applications of astigmatic quadrupole lenses in probe-forming systems when an elliptical or linear beam spot is needed rather than a round one [Baranova and Read 1998].

A short probe-forming system is developed for the Columbia microprobe includes four electrostatic quadrupoles with a Russian quadrupole configuration. The smallest beam spot size and appropriate optimal parameters of the probe-forming system had been found [Dymnikov and Brenner 2000]. The probe-forming system of a nuclear scanning microprobe based on the parametric multiplets of quadrupole lenses is optimized. The optimization is aimed at creating an ion probe with energy of several MeV that produces a micrometer spot on the target [Abramovich et al 2005].

Probe-forming quadrupole lens provides the following advantages; first, it permits variable spot – shaping by changing the lens excitation; second, the demagnification can be increased without increasing the working distance [Okayama 1989]. Angular aperture shaped beam system is the present invention provides improved angular aperture schemes for generating shaped beam spots having a desired geometric shape from rectangular, elliptical, and semi-elliptical apertures having one sharp edge. Depending on the particular beam spot that is desired, combinations of techniques including defocusing, aperture offsetting, and stigmatism adjustment, can be used in both spherical aberration dominant and chromatic aberration dominant environments to achieve a desired beam for a desired application [Gerlach et al 2001].

Quadrupole lens is necessary to produce a spatially linear electric field when focusing charge particle beams, deflecting polarized optical radiation in media with a linear electro-optical effect and in other applications [Norgorodtsev 1982]. There are many electron and ion optical instruments and devices in which there are advantages in using quadrupole lenses rather than round lenses, such as instruments where strong focusing or astigmatic properties are needed. Among these are accelerators, cathode – ray tubes, and devices for correcting aberrations [Baranova and Read 1998].

1-3 Historical Development

Melkich had been working in this field since 1944 pointed out the field properties of quadrupole numerous theoretical and experimental studies, but their practical application as system of cylindrical lenses data started only from 1952. The basic properties of quadrupole lenses had been presented in general form by Septier [1961] and Hawkes [1970]. Experiments on quadrupole lens system were reported by Septier [1958], Bauer [1965-6] Grewe et al [1967], Kawakatsu et al [1968] and Dhuiq [1968], according to Okayam and Kawakatsu in [1978].

Strashkevich [1963] investigated the spherical aberration for two limiting cases of the quadrupole lens: short lens and two dimensional. Hawkes [1967] calculated the real and virtual quadrupole aberration for system containing quadrupole lenses always forms virtual intermediate line images and each quadrupole is divergent in one plane. Hayashi and Sakudo [1968] calculated the fields in circular concave electrode with infinitesimal and infinite thickness analyzed by giving appropriate boundary conditions and calculated the optimum electrode angle. Results of calculations for spherical aberration of astigmatic doublet of quadrupole lenses for rectangular model had been compared with

spherical aberration of single quadrupole lens and axisymmetric magnetic lens by Fishkova and Yavor [1968].

Ovsyannikova and Yavor [1969] studied the potential distribution and focusing properties of asymmetrized quadrupole lenses with different electrode configuration. also, they calculated and measure different effective lengths for various electrode configurations like sphere, concave and convex cylindrical electrodes.

Markovich [1972] determined the short quadrupole, hexapole, and octupole lenses as aberration correctors for electron-beam deflection. Matsuda and Wollnik [1972] calculated the third – order transfer matrices for the fringing field of magnetic and electrostatic quadrupole lenses. Baranova et al [1972] determined the correction for the third – order geometric aberrations in symmetric quadrupole lens with concave electrodes.

SzaB`o [1973] described some results of the investigation of paraxial chromatic aberration of combined asymmetrized quadrupole lenses. Shott and Springer [1973] calculated and measured magnetic quadrupole lens with a large aperture and bell -shaped field distribution. Bosi [1974] investigated the two – dimensional equipotential model of circular concave quadrupole lenses . The exact solutions were carried out by the method of conformal mapping and expand in series of multiples.

Sakudo and Hayashi [1975] determined the fields formed with flat – face electrode by using conformal mapping. SzaB`o [1975] calculated the geometrical aberration combination of asymmetrically field quadrupole lenses and magnetic

sector. The potential distribution of circular concave 2N -electrodes and the optimum conditions had been discussed by Szilagyi [1976].

Okayama and Kawakatsu [1978] studied the potential distribution of quadrupole lens for circular electrodes using successive over – relaxation techniques involving the numerical solution of Laplace`s equation in three dimensions.

The resolution and chromatic aberration of a doublet of achromatic quadrupole lenses have been experimentally measured by Martin and Goloskie [1981]. Novgorodtsev [1982] considered that electric field strength distribution in quadrupole condensing lenses that have polygonal electrodes.

Okayama and Kawakatsu [1982] proposed a new electrostatic lens capable of correcting third-order aperture aberration. The new lens is called a self-aligned quadrupole correction lens and consists of an electrostatic quadrupole and an aperture electrode. Baranova and Yavor [1984] calculated the field of quadrupole lens of flat and circular concave electrodes. Jamieson and Legge [1988] discussed multipole lenses and how they might be used to correct divergence dependent aberration in quadrupole probe forming lens system.

Katsumi [1991] determined new normalization in optical properties of electrostatic quadrupole lens. Nakata [1993] studied numerically a new concave electrostatic lens with periodic electrode configuration. Baartman [1995] derived a simple formula for the aberrations due to the quadrupole finite length. It indicates that for fixed quadrupole center locations and focal strengths, longer quadrupole better. Baranova et al [1996] analysed the chromatic and aperture

aberrations of crossed five-aperture lenses by direct ray tracing. It was shown that in astigmatic modes the chromatic and aperture aberrations of one of the linear images can be simultaneously eliminated or made negative.

Baranova and Read [1998] determined the reduction of the chromatic and aperture aberrations of stigmatic quadrupole lens triplet. They calculated the minimization of the aberrations of electrostatic lens systems composed of quadrupole and octupole lenses.

Baranova and Read [1999] investigated and compared the aberrations for two types of multiplets based on electrostatic quadrupole and octupole lenses: mid-acceleration systems in which an accelerating potential was applied to the middle lenses of a set of quadrupole lenses and systems in which some of the quadrupole lenses were replaced by combined quadrupole-octupole lenses.

Dyminkov and Brenner [2000] were calculated the theoretical study of short electrostatic lens for the columbia ion microprobe. Shimizu et al. [2000] determined the characteristics of the beam line at the Tokyo electron beam ion trap. Filachevet et al. [2000] investigated the fifth order aperture aberration electrostatic quadrupole lens systems. Yamazaki et al. [2002] determined the electron optic using multipole lenses (i.e. quadrupole) for a low energy electron beam direct writing system Barnes et al. [2003] developed and characterized the electrostatic quadrupole extraction lens for mass spectrometry. An electrostatic quadrupole doublet with an integration steer was reported by Welsch et al. [2004].

Gillespie [2005] determined optics elements for modeling electrostatic lenses and accelerator components IV- electrostatic quadrupole and space charge

modeling. Dymanikov et al. [2005] determined zoom quadrupole focusing systems producing an image of an object. Rose et al. [2005] determined the spherical and chromatic aberration correction in electron microscopy .

1-4 Aim Of The Project

The present work aims at finding the optimum design of electrostatic quadrupole lens which give rise to the optimum value of spherical and chromatic aberration. Taking into consideration the cylindrical convex and spherical electrodes are generally used instead of hyperbolic electrodes because these electrodes are difficult to fabricate. The field distribution in electrostatic quadrupole lens depend on a large number of parameters, therefore in the present work we change the geometrical dimension of the electrode to find the optimum value of the lenses. The field model has been determined from the calculations of the potential distribution which is representing for each design of electrostatic quadrupole lens.

The some first order optical properties for each model will be computed by solving the trajectory equation of the charge-particles beam traversing in each field distribution, taking in to account the convergence and divergence planes. The effect of the electrodes shape (such as angle between the electrodes and radius of electrode to aperture radius ratio) on the focal length, magnification, spherical and chromatic aberration coefficients will be investigated in detail to

find the optimum value for these properties for each design of electrostatic quadrupole lens.

2- PROPERTIES OF ELECTROSTATIC QUADRUPOLE LENS FOR DIFFERENT ELECTRODE SHAPE

2-1 The Electrode Shape of Quadrupole Lens

Hyperbolic electrode are well known as being useful for creating an ideal configuration for quadrupole field in a two – dimensional and three – dimensional approximation because these electrodes are difficult to fabricate and it is difficult to achieve the required curvilinear form, and the width and distance between electrode of opposite polarity are finite, which causes distortions in the field, rod –type electrodes (like cylindrical, circular or spherical electrodes), or polygonal electrodes are generally used instead [Nakata 1993].

The electric field strength distribution in quadrupole condensing lenses with polygonal and rod – type are easier to calculated than hyperbolic electrodes and give strictly linear field distribution . The electrode profile is chosen to cancel the terms in the power series expansion of the complex field potential near the center of the system. The distribution of the field intensity gradient non uniformities is investigated quadrupole condensing lenses having simpler electrode (plates, angle, cylindrical, spherical surfaces) [Novgorodtsev 1982].

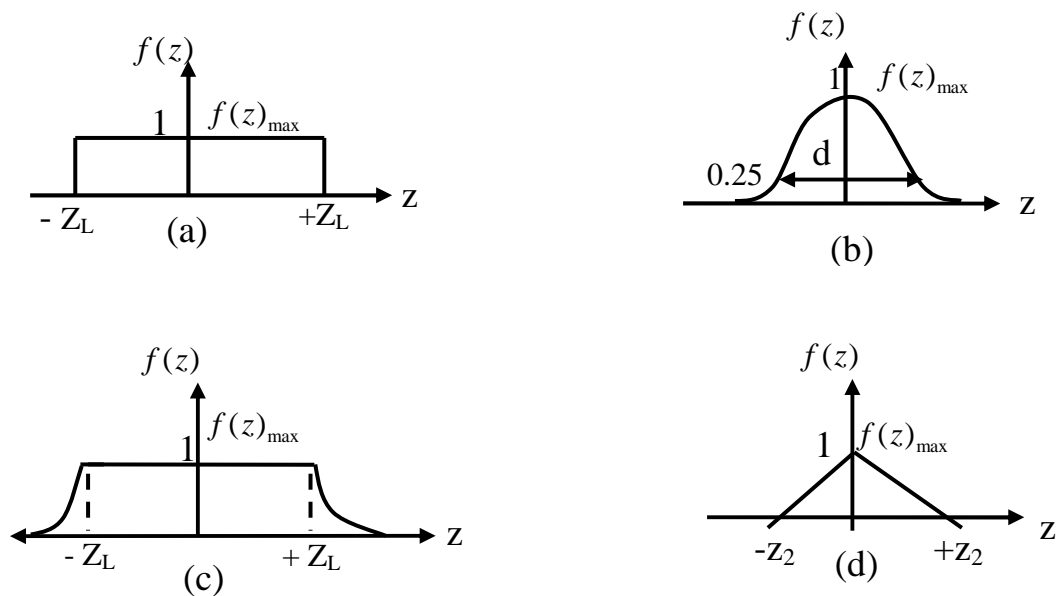
The field distribution in electrostatic quadrupole lens depend on a large number of parameters : electrode voltage ratios, aperture size, electrode thicknesses and spacings between them ,as well as the radial and longitudinal dimensions of the electrode. The particular electrode configuration may result in a single value of K [Szilagyi 1988]. The potential distribution model and the focal properties of quadrupole lenses in the form of comprehensive data directly related to the lens geometries, (i.e. electrode shape of lens) and

excitations. The field model is determined from the calculations of the potential distribution [Okayama and Kawakatsu 1978].

2-2 Field Models For Quadrupole Lenses

The field distribution of a quadrupole lens may be represented by various models shown in figure (2-1). These potential distribution models are actually proposed for the cross-section of the quadrupole lens electrodes [Hawkes 1965/1966]. According to Hawkes the function $f(z)$ of the field distribution can be obtained either by measurement or by computation, some mathematically convenient models may be transpired $f(z)$ sufficiently.

For example, for long narrow quadrupole lenses, the rectangular model figure (2-1-a) is often a close enough approximation;



Figure(2-1):Field distribution of a quadrupole lens (Hawkes1965/1966).

(a) Rectangular model

(b) Bell-shaped model

(c) Modified bell-shaped model

(d) Triangular model

The function $f(z)$ for a rectangular field model of long quadrupole is represented in the following form:

$$f(z) = f(z)_{\max} = 1 \quad \text{when } -z_L \leq z \leq z_L \quad (2-1)$$

At points when $|z| > z_L$ the function $f(z) = 0$, where z_L equal to $L/2$. This model is also known as the square-top field distribution. The length L is the “effective length”.

For short quadrupole lens, Glaser's bell-shaped field model shown in figure (2-1-b) is found to be more suitable and is represented by the following function [Hawkes 1970]:

$$f(z) = f(z)_{\max} / [1 + (z/d)^2]^2 = 1 / [1 + (z/d)^2]^2 \quad (2-2)$$

d = the axial extension of the field between the two points where $f(z) = f(z)_{\max} / 4$; at $z = 0$, $f(z)_{\max}$ equals to unity.

The modified bell-shaped field model shown in figure (2-1-c) represents the intermediate case between the rectangular and the bell-shaped model such that the field distribution may be represented by the following function:

$$f(z) = 1 / [1 + ((z - z_L)/d)^2]^2 \quad \text{when } z > z_L \quad (2-3)$$

$$f(z) = 1 / [1 + ((z + z_L)/d)^2]^2 \quad \text{when } z < -z_L \quad (2-4)$$

The function $f(z)$ has a rectangular section of constant maximum value $f(z)_{\max} = 1$ in the region $-z_L \leq z \leq z_L$ such that beyond these boundaries it terminates in the form of a half bell-shaped field represented by equations (2-3) and (2-4).

The triangular field distribution model shown in figure (2-1-d) is another model proposed by Hawkes [1965/1966]; it is given by:

$$f(z) = \lambda z + z_2 \quad \text{when } -z_2 \leq z \leq 0 \quad (2-5-a)$$

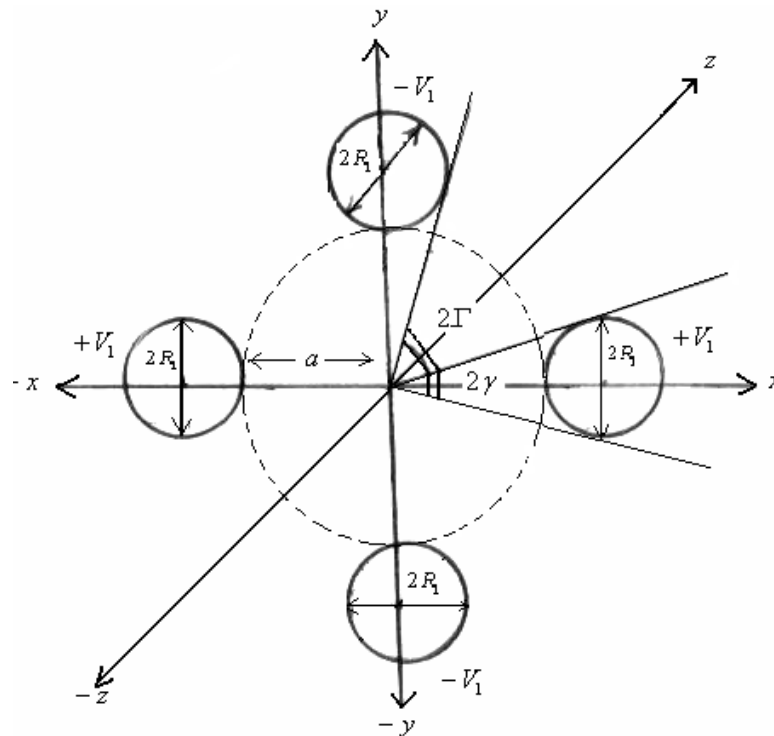
$$f(z) = -\lambda z + z_2 \quad \text{when } 0 \leq z \leq z_2 \quad (2-5-b)$$

$$f(z) = f(z)_{\max} = 1 \quad \text{at } z = 0 \quad (2-5-c)$$

where λ is the slope of the two steep sides of the triangle and equal unity.

2-3 Quadrupole Field in Cylindrical Convex Electrodes.

The electrode configuration consisting of four symmetrically convex cylindrical quadrupole lens as shown in Figure (2-2). In this figure γ and Γ are half of the electrode angle and half of the gap angle respectively.



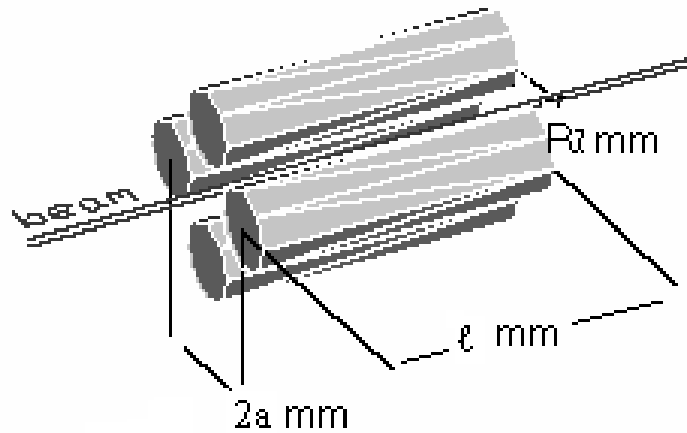
Figure(2-2): Quadrupole electrodes of cylindrical convex electrode [Strashkevich 1963].

The effective length L had been found experimentally to be given by [Kiss et al. 1969] :

$$L = \ell + 1.056 a \quad (2-6)$$

$$R_1 = c a \quad (2-7)$$

where ℓ is the electrode length and c is constant relative between the radius of cylindrical convex R_1 and the aperture radius a as in figure (2-3).



Figure(2-3): Electrodes of quadrupole lens, cylindrical convex Electrodes.

In order to obtain the optimum electrode angle 2γ , it is necessary to analyze the field formed by this electrode system. The potential distribution of a quadrupole lens with cylindrical electrodes was calculated by solution of Laplace's equation in three dimension . The result shows that the modified bell-shaped is very close approximation to the potential function for the relatively long quadrupole lens $\ell \gg a$. The solution of $V(r, \theta, z)$ is thus expressed as [Hayashi and Sakudo 1968]:

$$V(r, \theta, z) = D_0(z) V_1 (r/a)^2 \cos(2\theta) + D_1(z) V_1 (r/a)^6 \cos(6\theta) + D_2(z) V_1 (r/a)^{10} \cos(10\theta) + \dots + D_n(z) V_1 (r/a)^{2(2n+1)} \cos(2((2n+1)\theta)) \quad (2-8)$$

The first term ($n=0$) of equation (2-8) is the ideal quadrupole field component and the others are the higher spatial harmonic components. The second and the third terms ($n=1,2$) correspond to 12- and 20- electrode field components respectively. The best approximation for getting a quadrupole field is achieved practically if the ($n=1$) and higher terms component is eliminated :

$$V(r, \theta, z) = D(z) V_1 (r/a)^2 \cos(2\theta) \quad (2-9)$$

$$D(z) = K f(z) \quad (2-10)$$

Where V_1 is the potential of the electrode, and the form of the $f(z)$ function normalized to unity (at the center $z=0$) and K are determined by the electrode geometry (electrode shape).

The value of K which was represented by the following function for cylindrical convex electrodes [Strashkevich 1963]:

$$K = 2 \sin(2\Gamma) / \ln(R_1/a) \quad (2-11)$$

The expression of potential distribution in equation (2-8) in cylindrical coordinates can be expressed in Cartesian coordinates as shown below:

$$r^{2n} = (x^2 + y^2)^n, \text{ then one can simply write} \quad (2-12)$$

$$r = (x^2 + y^2)^{1/2} \quad (2-13)$$

By using the following expressions [Szilagyi 1988]:

$$r^2 \cos(2\theta) = (x^2 - y^2) \quad (2-14)$$

$$r^6 \cos(6\theta) = x^6 - y^6 - 3(x^4 y^2 - x^2 y^4) \quad (2-15)$$

$$r^{10} \cos(10\theta) = x^{10} - y^{10} - 45(x^8 y^2 - x^2 y^8) + 210(x^6 y^4 - x^4 y^6) \quad (2-16)$$

With the relationship given by equation (2-14) to (2-16) and substituting in equation (2-8) one can get the general expression for the potential distribution in Cartesian coordinates [Grivet 1972]:

$$\begin{aligned} V(x, y, z) = & D_0(z) V_1(x^2 - y^2) / a^2 + D_1(z) V_1(x^6 - y^6 - 3(x^4 y^2 - x^2 y^4)) / a^6 + \\ & D_2(z) V_1(x^{10} - y^{10} - 45(x^8 y^2 - x^2 y^8)) / a^{10} + 210(x^6 y^4 - x^4 y^6) + \dots \end{aligned} \quad (2-17)$$

2-4 Quadrupole Field in Spherical Electrodes.

The electrostatic quadrupole lens has constructed from four spheres of small radius relative to the aperture a as figure (2-4). Considering the electrode configuration as composed of four point charges closed with spheres of small radius b . For the paraxial region the field distribution can be fitted with a curve of the bell – shaped field model type. The z_1 and b (given in the units of aperture radius) parameters ($z_L = 0$) as well as the effective length formulae obtained by [Kiss et al. 1969]:

$$L = 1.32 a \quad (2-18)$$

$$b = I a \quad (2-19)$$

where I is constant relative between the radius of spherical electrode b and the aperture radius a as in figure (2-4).

The equations of field distribution for spherical electrodes is the same as (2-8) to (2-17) except equation (2-11) because the value of K which is represented by the following function [Strashkevich 1963]:

$$K = 3 a^4 b \sin(2\Gamma) (a^2 + L^2)^{-5/2} \quad (2-20)$$

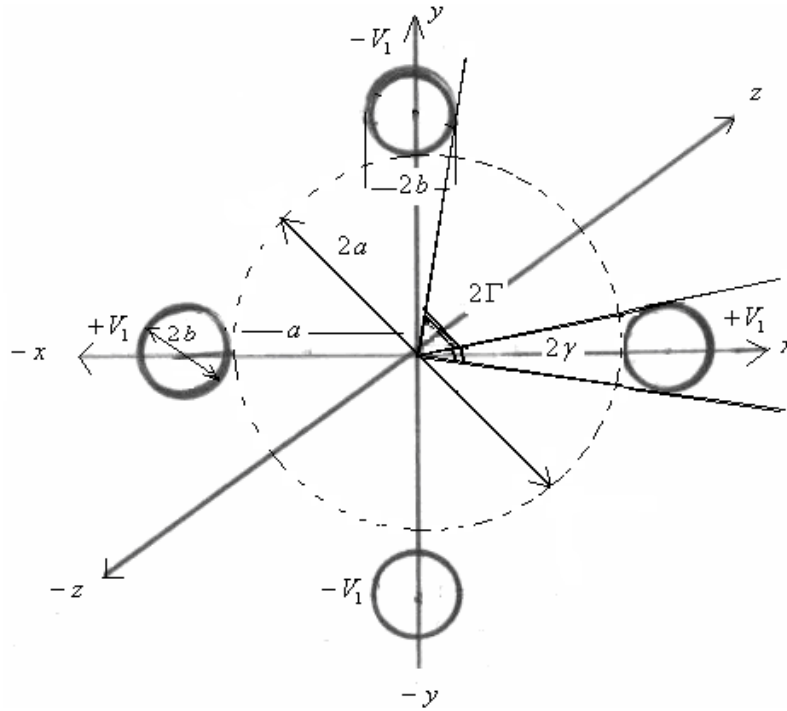


Figure (2-4): spherical electrodes of quadrupole lens [Strashkevich 1963].

2-5 First–Order Optical Properties for an Electrostatic

Quadrupole Lens:

2-5-1 The equation of motion

The trajectory equations in Cartesian coordinates for the charged – particles beam traversing the field of a quadrupole lens are given as follows [Hawkes 1970]

$$x'' + \beta^2 f(z)x = 0 \quad (2-21)$$

$$y'' - \beta^2 f(z)y = 0 \quad (2-22)$$

where β is the excitation parameter, given by the following relation:

$$\beta^2 = V_1 K / a^2 V_0 \quad (2-23)$$

where V_1 being the electrode voltage, v_0 acceleration voltage, x'' and y'' are the second derivatives with respect to z , and K is a coefficient accounting for the shape of electrodes. Since the present work has been concentrated on the cylindrical convex shape for the electrodes, [Dymnikov et al. 1965 and Grivet 1972].

By using equations (2-21) and (2-22) yield with equation (2-3) which represented the field for cylindrical electrode shape :

$$x'' + \beta^2 x / [1 + ((z - z_L) / d)^2]^2 = 0 \quad (2-24)$$

$$y'' - \beta^2 y / [1 + ((z - z_L) / d)^2]^2 = 0 \quad (2-25)$$

Let the new variables P and ψ be introduced, so that one would have by Hawkes [1967] :

$$(z - z_L) / d = \cot(\psi) \quad (2-26)$$

and

$$x / d = P(\psi) / \sin(\psi) \quad (2-27)$$

then equation (2-24) for convergence plane can be rewritten as :

$$d^2 P / d\psi^2 + W_x^2 P = 0 \quad (2-28)$$

and equation (2-25) for divergence plane can be rewritten as :

$$d^2 P / d\psi^2 - W_y^2 P = 0 \quad (2-29)$$

The properties of the quadrupole lens are characterized by the parameter:

$$W_x = 1 - \beta^2 d^2 \quad \text{for the convergence plane}$$

$$W_y = 1 + \beta^2 d^2 \quad \text{for the divergence plane}$$

The solution of equations (2-24) and (2-25) is elementary.

Returning to the variables x and y one can write:

$$x = d [x_0 \cos(W_x \psi) + x_0' \sin(W_x \psi)] / \sin(\psi) \quad (2-30)$$

Similarly for y but replacing W_x by W_y

$$y = d [y_0 \cos(W_y \psi) + y_0' \sin(W_y \psi)] / \sin(\psi) \quad (2-31)$$

$$\begin{aligned} x' = \{ & x_0 [d W_x \sin(\psi) \sin(W_x \psi) + d \cos(\psi) \cos(W_x \psi)] / \sin^2(\psi) [1 + ((z - z_1) / d)^2 \\ & d] + \{ x_0' [d \cos(\psi) \sin(W_x \psi) - d W_x \sin(\psi) \cos(W_x \psi)] / \sin^2(\psi) [1 + ((z - z_1) \\ & / d)^2 d] \} \end{aligned} \quad (2-32)$$

and similarly for y :

$$\begin{aligned} y' = \{ & y_0 [d W_y \sin(\psi) \sin(W_y \psi) + d \cos(\psi) \cos(W_y \psi)] / \sin^2(\psi) [1 + ((z - z_1) / d)^2 \\ & d] + \{ y_0' [d \cos(\psi) \sin(W_y \psi) - d W_y \sin(\psi) \cos(W_y \psi)] / \sin^2(\psi) [1 + ((z - z_1) \\ & / d)^2 d] \} \end{aligned} \quad (2-33)$$

where x_o and y_o are the initial displacements from the optical axis in the $x-z$ and $y-z$ plane respectively, and x'_o and y'_o are the initial gradients of the beam in the corresponding planes.

The general solution of the second-order linear homogeneous differential equations (2-24) and (2-25) can always be written in the following matrix form respectively.

$$\begin{pmatrix} x(z) \\ x'(z) \end{pmatrix} = T_x \begin{pmatrix} x_o(z) \\ x'_o(z) \end{pmatrix} \quad (2-34)$$

$$\begin{pmatrix} y(z) \\ y'(z) \end{pmatrix} = T_y \begin{pmatrix} y_o(z) \\ y'_o(z) \end{pmatrix} \quad (2-35)$$

The parameters T_x and T_y are the transfer matrices in the convergence plane xOz and the divergence plane yOz respectively which are given by Larson [1981] and Szylagyi [1988]:

$$T_x = \begin{pmatrix} \frac{d \cos(W_x \psi)}{\sin(\psi)} & \frac{d \sin(W_x \psi)}{\sin(\psi)} \\ \frac{d W_x \sin(\psi) \sin(W_x \psi) + d \cos(\psi) \cos(W_x \psi)}{\sin^2(\psi) [1 + (z - z_L/d)^2] d} & \frac{d \cos(\psi) \sin(W_x \psi) - d W_x \sin(\psi) \cos(W_x \psi)}{\sin^2(\psi) [1 + (z - z_L/d)^2] d} \end{pmatrix} \quad (2-36)$$

$$T_y = \begin{pmatrix} \frac{d \cos(W_y \psi)}{\sin(\psi)} & \frac{d \sin(W_y \psi)}{\sin(\psi)} \\ \frac{d W_y \sin(\psi) \sin(W_y \psi) + d \cos(\psi) \cos(W_y \psi)}{\sin^2(\psi)[1+(z-z_L/d)^2]d} & \frac{d \cos(\psi) \sin(W_y \psi) - d W_y \sin(\psi) \cos(W_y \psi)}{\sin^2(\psi)[1+(z-z_L/d)^2]d} \end{pmatrix} \quad (2-37)$$

All first-order optical properties of a quadrupole lens can be derived from the matrices given in equations (2-36) and (2-37). These matrices are represented by Regenstreif [1967] :

$$T = \begin{pmatrix} a_{11} & a_{12} \\ a_{21} & a_{22} \end{pmatrix} \quad (2-38)$$

2-5-2 The focal lengths

The focal length is defined as the distance between the focal point and the corresponding principal plane. Therefore, the image- and object-side focal lengths f_i and f_o respectively are given by :

$$f_i = f_o = -1/a_{21} \quad (2-39)$$

$$f_x = -\frac{\sin^2(\psi) [1+(z-z_L/d)^2] d}{[d W_x \sin(\psi) \sin(W_x \psi) + d \cos(\psi) \cos(W_x \psi)]} \quad (2-40)$$

$$f_y = -\frac{\sin^2(\psi) [1+(z-z_L/d)^2] d}{[d W_y \sin(\psi) \sin(W_y \psi) + d \cos(\psi) \cos(W_y \psi)]} \quad (2-41)$$

2-5-3 The magnification

In any optical system the ratio between the transverse dimension of the final image and the corresponding dimension of the original object is called the magnification M given as:

$$M = 1 / (a_{21} u + a_{11}) \quad (2-42)$$

where u is the object distance.

$$M_x = \frac{1}{\frac{dW_x \sin(\psi) \sin(W_x \psi) + d \cos(\psi) \cos(W_x \psi)}{\sin^2(\psi)[1 + (z - z_L / d)^2]d} u + \frac{d \cos(W_x \psi)}{\sin(\psi)}} \quad (2-43)$$

$$M_y = \frac{1}{\frac{dW_y \sin(\psi) \sin(W_y \psi) + d \cos(\psi) \cos(W_y \psi)}{\sin^2(\psi)[1 + (z - z_L / d)^2]d} u + \frac{d \cos(W_y \psi)}{\sin(\psi)}} \quad (2-44)$$

Furthermore, in the case of spherical electrode shape (which is represented by the bell-shaped field model) the above expressions are applied in both convergence and divergence plane provided that z_L any where in above equations is replaced by zero ($z_L = 0$).

2-6 Lens Aberrations

The discussion of image formation has been confined so far to paraxial conditions, in which contributory rays make with the axis an angle so small that its value (in radian measure) is not significantly different from that of the sine. In such a case all rays from a given point of the object come together again in a single point of the image ; the object gives a true image , which is then said to be aberration-free [Cosslett 1950].

The aberration is a subject of great importance, in general the image will suffer from varying proportions of all the aberrations, and consequently will exhibit greater or less confusion. For these rays the value of the sine of the angle approximates closely to that obtained from the first two terms in the series [Cosslett 1950] :

$$\sin(\theta) = \theta - \theta^3/3! + \theta^5/5! - \dots \quad (2-45)$$

Under these condition it is found that the image is more or less seriously distorted with respect to the object: electrons from the same point on the object intersect the image plane in different points, and the image plane itself may be curved. The variation in the position of the image that is found for electrons of varying velocities (chromatic aberration) requires separate treatment. An optical system is said to suffer from spherical aberration when rays incident at varying radial distances are focused to different points on the axis [Hawkes 1973].

Aberration is not the only defect that the image suffers from. Other type of defects are due to the fabrication of lenses such as mechanical imperfection and misalignment. The electrostatic repulsion forces between particles of the same charge causes a deviation in charged particles path. It is another defects, known

as the space charge effect, and it is a case of charged-particle optics alone that cannot be found in light optics [Szilagyı 1988].

Spherical and chromatic aberrations limit the resolution of conventional electron microscopes. This behavior differs in rotational symmetry from that of a multipole because its potential adopts at the boundary either a maximum or a minimum depending on the polarity of the potential at the electrode or pole piece, respectively. This is the reason why we can compensate for the spherical aberration by abandoning rotational symmetry [Rose et al. 2005].

However, in the present work attention is paid only on the two main aberrations, namely spherical aberration and chromatic aberration of electrostatic quadrupole lenses due to their significant effect in various ion and electron optical systems.

2-6-1 Spherical aberration of a quadrupole lens

Spherical aberration in a lens prevents all the rays from meeting at the same focal point, which causes images to become blurred. The deviation of an electron in the case of an electron microscope is proportional to the height of the ray from the optic axis, and the deflection is always in the direction towards the optic axis. It is also called aperture aberration. In a quadrupole lens, the spherical aberration in the Gaussian image plane can be expressed as (Hawkes 1970 and Okayama 1989):

$$\Delta x(zi) = M_x (C_{30} \alpha^3 + C_{12} \alpha \delta^2) \quad (2-46)$$

$$\Delta y(zi) = M_y (D_{21} \alpha^2 \delta + D_{03} \delta^3) \quad (2-47)$$

where α and δ are the image side semi-aperture angles in the x-z and y-z plane respectively, The coefficients C characterize the aberration in the convergence plane, and D in the divergence plane. The coefficient C_{30} determines the aberration of the real width image in the plane $y = 0$, and D_{03} is that for the imaginary image in the plane of $x = 0$. And the value of ψ_0 corresponds to the position of the object and ψ_1 to that of the image, and ($n = -1$) for electrostatic quadrupole lens [Fishkova et al. 1968].

The spherical aberration coefficients C and D are determined from the relations given in [Dymnikov et al. 1965].

$$\begin{aligned} \frac{C_{30}}{d} = & \frac{1}{32 \sin^4 \psi_0} [(w_x^2 - 1)(w_x^2 + 3) \frac{\pi}{w_x^5} + \frac{2(7 - w_x^2)}{4w_x^2 - 1} (\sin 2\psi_0 - \sin 2\psi_1) + (2 - 2n + 3n^2) \\ & (w_x^2 - 1) [(w_x^2 - 1) \frac{\pi}{w_x^5} - \frac{2}{4w_x^2 - 1} (\sin 2\psi_0 - \sin 2\psi_1)]] \end{aligned} \quad (2-48)$$

$$\begin{aligned} \frac{C_{12}}{d} = & \frac{1}{32 w_y^2 \sin^4(\psi_0)} [[-4[(1 - \cos(2\pi \frac{w_y}{w_x})) \sin(2\psi_1) + w_y(1 - \cos(2\psi_1) \sin(2\pi \frac{w_y}{w_x}))] \\ & + 3(w_x^2 - 1)[-2(w_x^2 - 1) \frac{\pi}{w_x^3} + \frac{1}{w_x^2 - 1} [-\frac{w_y^2(w_x^2 w_y^2 + 2)}{4w_x^2 w_y^2 - 1} \sin(2\psi_0) + (w_y^2 + 3) \\ & \sin(2\psi_1) + \frac{3w_y^2 + 1}{2w_y} \sin(2\pi \frac{w_y}{w_x})] - \frac{3}{4w_x^2 w_y^2 - 1} [(4w_y^2 - 1) \sin(2\psi_1) \cos(2\pi \frac{w_y}{w_x}) \\ & + w_y(2w_y^2 + 1) \cos(2\psi_1) \sin(2\pi \frac{w_y}{w_x})]] + (2 + 2n - n^2) (w_x^2 - 1) [2(w_x^2 - 1) \frac{\pi}{w_x^3} - \\ & \frac{4w_y^2(w_x^2 - 1)}{4w_x^2 w_y^2 - 1} \sin(2\psi_0) + \sin(2\psi_1) - \frac{1}{2w_y} \sin(2\pi \frac{w_y}{w_x}) - \frac{1}{4w_x^2 w_y^2 - 1} [(4w_y^2 - 1) \\ & \sin(2\psi_1) \cos(2\pi \frac{w_y}{w_x}) + w_y(2w_y^2 + 1) \cos(2\psi_1) \sin(2\pi \frac{w_y}{w_x})]]]] \end{aligned} \quad (2-49)$$

$$\begin{aligned}
\frac{D_{03}}{d} = & \frac{w_x^2 - 1}{32 w_y^4 \sin^4(\psi_0)} \left[-\frac{1}{3} [2(2+n)w_y(1 - \cos(2\psi_1))(1 - \cos(2\pi \frac{w_y}{w_x})) \sin(2\pi \frac{w_y}{w_x}) \right. \\
& + (4-n)(\cos(4\pi \frac{w_y}{w_x}) - 4\cos(2\pi \frac{w_y}{w_x}) + 3) \sin 2\psi_1] - (w_y^2 + 3) \frac{\pi}{w_x} + \\
& \frac{2w_y^4(5+w_x^2)}{(w_x^2-1)(4w_y^2-1)} \sin(2\psi_0) + \frac{1+w_x^2}{2} \sin(2\psi_1) + \frac{2}{w_y} \sin(2\pi \frac{w_y}{w_x}) - \frac{w_x^2-1}{4w_y} \\
& \sin(4\pi \frac{w_y}{w_x}) - \frac{2}{w_x^2-1} [(w_y^2+1) \sin(2\psi_1) \cos(2\pi \frac{w_y}{w_x}) + 2w_y(\cos 2\psi_1) \\
& \sin(2\pi \frac{w_y}{w_x})] - \frac{1}{2(4w_y^2-1)} [(5w_y^2+1) \sin(2\psi_1) \cos(4\pi \frac{w_y}{w_x}) + 2w_y(w_y^2+2) \\
& \cos(2\psi_1) \sin(4\pi \frac{w_y}{w_x})] + \frac{1}{3} (2-2n+3n^2)(w_x^2-1) [\frac{3\pi}{w_x} + \frac{6w_y^4}{(w_x^2-1)(4w_y^2-1)} \\
& \sin(2\psi_0) + \frac{2}{3} \sin(2\psi_1) - \frac{2}{w_y} \sin(2\pi \frac{w_y}{w_x}) + \frac{1}{4w_y} \sin(4\pi \frac{w_y}{w_x}) - \frac{2}{w_x^2-1} (\sin(2\psi_1) \\
& \cos(2\pi \frac{w_y}{w_x}) + w_y \cos(2\psi_1) \sin(2\pi \frac{w_y}{w_x})) - \frac{1}{2(4w_y^2-1)} (\sin(2\psi_1) \cos(4\pi \frac{w_y}{w_x}) \\
& \left. + 2w_y \cos(2\psi_1) \sin(4\pi \frac{w_y}{w_x})) \right]
\end{aligned} \tag{2-50}$$

$$\begin{aligned}
\frac{D_{21}}{d} = & \frac{C_{12}}{d} - \frac{1}{8 w_y^2 \sin^4(\psi_0)} [(1 - \cos(2\pi \frac{w_y}{w_x})) \sin(2\psi_1) + w_y (1 - \cos(2\psi_1)) \\
& \sin 2\pi \frac{w_y}{w_x}]
\end{aligned} \tag{2-51}$$

2-6-2 Chromatic aberration of a quadrupole lens

The first – order axial chromatic aberration, which cannot be compensated in rotationally symmetric systems. In such systems the faster electrons will always be less focused than the slower ones [Hawkes 1973]. In order that the influence of chromatic aberration as well as nonlinear image fields may be minimized, some design constraints are imposed on the maximum radius of the beam, dimensions of the quadrupole lens, and applied voltage on the quadrupole [Guharay et al. 2001].

In a quadrupole lens, the chromatic aberration in the Gaussian image plane can be expressed as (Hawkes 1970):

$$\Delta x(z_i) = M_x (C_{cx} \alpha + C_{mx} x_o) \frac{V(r, \theta, z)}{V_o} \quad (2-52)$$

$$\Delta y(z_i) = M_y (C_{cy} \delta + C_{my} y_o) \frac{V(r, \theta, z)}{V_o} \quad (2-53)$$

where α and δ are the image side semi-aperture angles in the x-z and y-z plane, respectively.

The coefficients of chromatic aberration $C_{cx}, C_{cy}, C_{mx}, C_{my}$ are given by [Hawkes 1970]:

$$\frac{C_{cx}}{d} = \frac{n-1}{8} \frac{\beta^2 d^2}{\sin(\pi w_x)^2} \left[\left(\frac{\sin(2\pi w_x)}{w_x} - 2\pi \right) (m_x^2 + 1) + 4m_x \left(\frac{\sin(\pi w_x)}{w_x} - \pi \cos(\pi w_x) \right) \right] \quad (2-54)$$

$$\frac{C_{cy}}{d} = \frac{n-1}{8} \frac{\beta^2 d^2}{\sin(\pi w_y)^2} \left[\left(\frac{\sin(2\pi w_y)}{w_y} - 2\pi \right) (m_y^2 + 1) + 4m_y \left(\frac{\sin(\pi w_y)}{w_y} - \pi \cos(\pi w_y) \right) \right] \quad (2-55)$$

$$C_{mx} = \frac{n-1}{8} \frac{\beta^2 d^2 f_x}{w_x^2 d} \left[\left(\frac{\sin(2\pi w_x)}{w_x} - 2\pi \right) m_x + 2 \left(\frac{\sin(\pi w_x)}{w_x} - \pi \cos(\pi w_x) \right) \right] \quad (2-56)$$

$$C_{my} = \frac{n-1}{8} \frac{\beta^2 d^2 f_y}{w_y^2 d} \left[\left(\frac{\sin(2\pi w_y)}{w_y} - 2\pi \right) m_y + 2 \left(\frac{\sin(\pi w_y)}{w_y} - \pi \cos(\pi w_y) \right) \right] \quad (2-57)$$

2-7 Computer program for computing the beam trajectory, the optical properties and the aberration coefficients of electrostatic quadrupole lens

A computer program with MathCAD professional 2001i has been used for determining the trajectory of charged particles traversing the field of electrostatic quadrupole lens in both the convergence plane and divergence plane, by using the transfer matrices given in equations (2-36) and (2-37) where the axial potential field has been computed to have a field model which close to its distribution.

The first order optical properties such as the focal length and magnification have been computed with the aid of equations (2-40) to (2-44) in the planes of convergence and divergence. The spherical aberration coefficients C_{30} , C_{12} , D_{03} , and D_{21} and chromatic aberration coefficients C_{cx} , C_{cy} , C_{mx} , and C_{my} are computed by using equations (2-48) to (2-57) for each design of electrostatic quadrupole lens. Figure (2-5) illustrates a block diagram of this computer program.

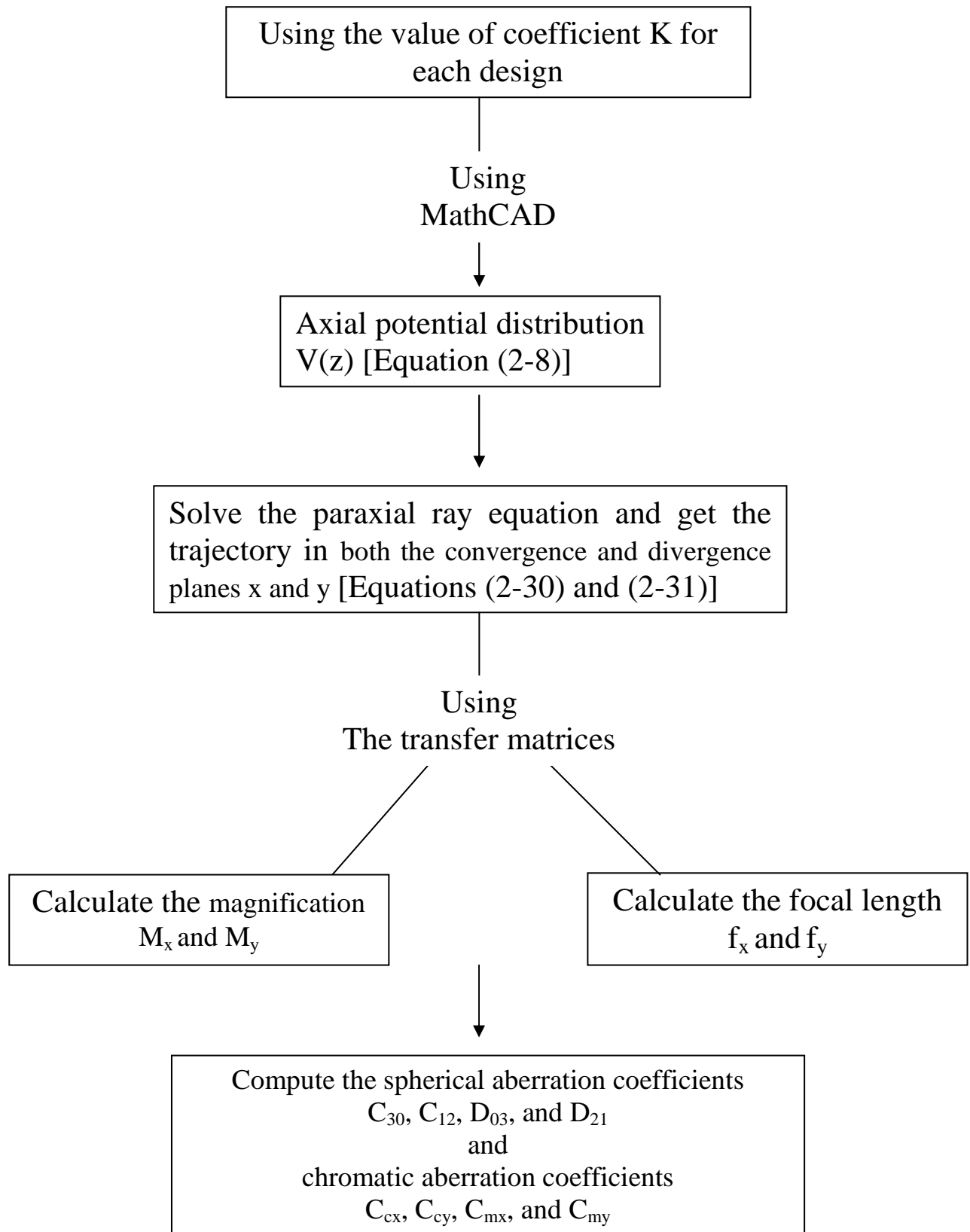


Figure (2-5): A block diagram of the MathCAD program for computing, the axial potential distribution, the trajectory, the optical properties and the aberration coefficients of electrostatic quadrupole lens.

3- RESULTS AND DISCUSSION

3-1 Introduction

The purpose of present work is finding the optimum design of electrostatic quadrupole lens which give rise to the optimum value of properties. The two types of electrodes cylindrical convex electrodes and spherical electrodes are used to find optimum field model which is close to the field distribution for each design of the lens. The path of charge-particles beam traversing the field model have been determined by using the solution of the trajectory equation of motion in Cartesian coordinates.

The optimization is made in each model by solving the equation of motion and finding the transfer matrices in convergence and divergence planes, which are used to find optimum values of the properties of each lens design as focal length, magnification, spherical aberration coefficients, and chromatic aberration coefficients. The optimization for cylindrical convex electrodes and spherical electrodes are made by changing the geometrical shape of the electrodes for each design such as; varying the gap angle between electrodes where the relative electrode radius to aperture radius ratio is varied.

3-2 Cylindrical Convex Electrodes

3-2-1 The potential distribution

The quadrupole lens is taken into account to the focusing of an accelerated charge- particles beam traveling from left to right - hand – side . The potential distribution of electrostatic quadrupole lens depend on many parameters for each design, such as for cylindrical convex electrodes depend on aperture radius $a=3mm$, electrode length $\ell = 6mm$, effective length L which is given by

equation (2-6), radius of electrode R_1 which is given by equation (2-7), and the gap angle 2Γ between the electrodes (see figures (2-2) and (2-3)).

Equation (2-8) gives the potential along the optical axis in terms of electrode voltage V_1 , electrode shape K , and the aperture radius a . The variation of the parameter K according to electrode shape gives different shape of potential distribution.

Figure (3-1) shows the axial potential distribution ratio ($V(z)/V_1$) based on the expression given in equation (2-9), it is found that very close to modified bell-shaped model by use quadrupole lens of cylindrical convex. This result is in agreement with the results mentioned in various references (see for example Kiss et al. 1970).

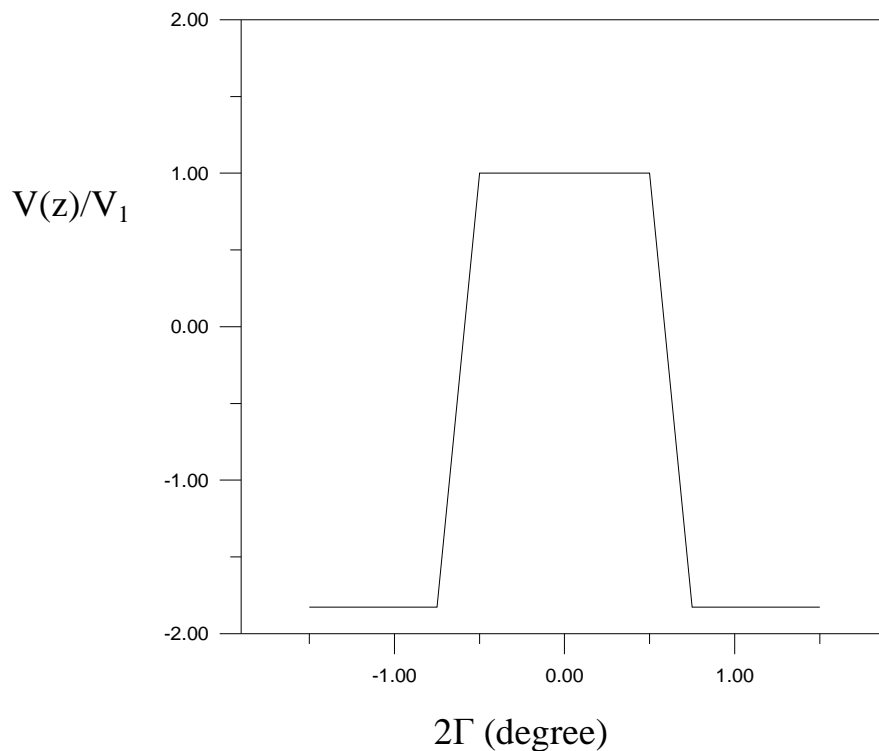
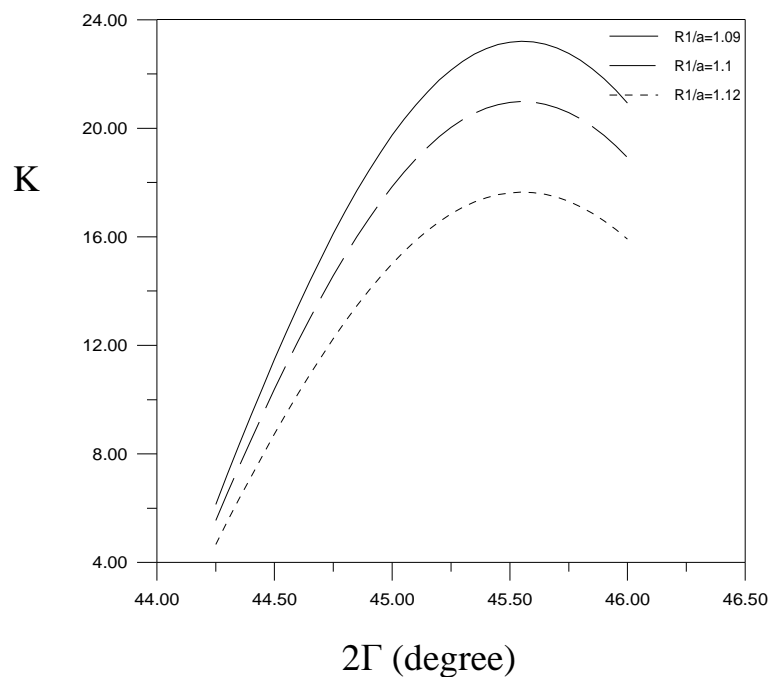


Figure (3-27): The relative spherical aberration coefficient D_{03}/d of electrostatic quadrupole lens with spherical electrodes as a function of gap angle 2Γ for three values of $b/a = 0.4, 0.425, \text{ and } 0.45$.

The radius R_1 of the electrodes was altered so that the value of R_1/a varied in the interval $1.00 \leq R_1/a \leq 1.25$, the value of $R_1/a = 1.09, 1.1, \text{ and } 1.12$ have been determined by the trial -and- error method where the lowest possible aberrations were achieved. The value of 2Γ varied in the interval $44.25^\circ \leq 2\Gamma \leq 46.20^\circ$. The coefficients K and β are calculated from equations (2-11) and (2-23) respectively for each value of R_1/a and 2Γ at constants aperture radius $a = 3 \text{ mm}$, electrode voltage $V_1 = 100 \text{ volt}$, and accelerating voltage $V_o = 10 \text{ k volt}$.

The results of the K and β are plotted in figures (3-2) and (3-3), respectively, these coefficient are plotted against 2Γ for several values of $R_1/a = 1.09, 1.1, \text{ and } 1.12$. It can be seen that, for low values of the angle 2Γ , all curves have slightly difference in K values. When the angular distance 2Γ between the electrodes increases the difference in values of K will be greater. All curves in these figures the value of K and β increases with increasing 2Γ reaching a maximum values at $2\Gamma = 45.5^\circ$ beyond this angle the curves decreases with increasing 2Γ .



Figure(3-2): The coefficient of electrode shape K for electrostatic quadrupole lens with cylindrical convex electrodes as a function of gap angle 2Γ for three values of $R_1/a = 1.09, 1.1, \text{ and } 1.12$.

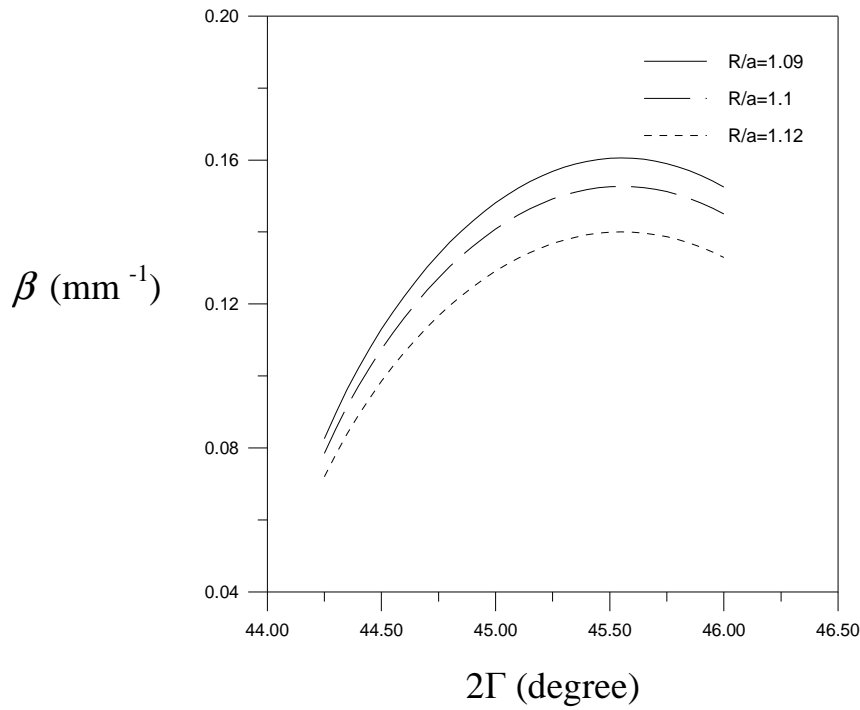


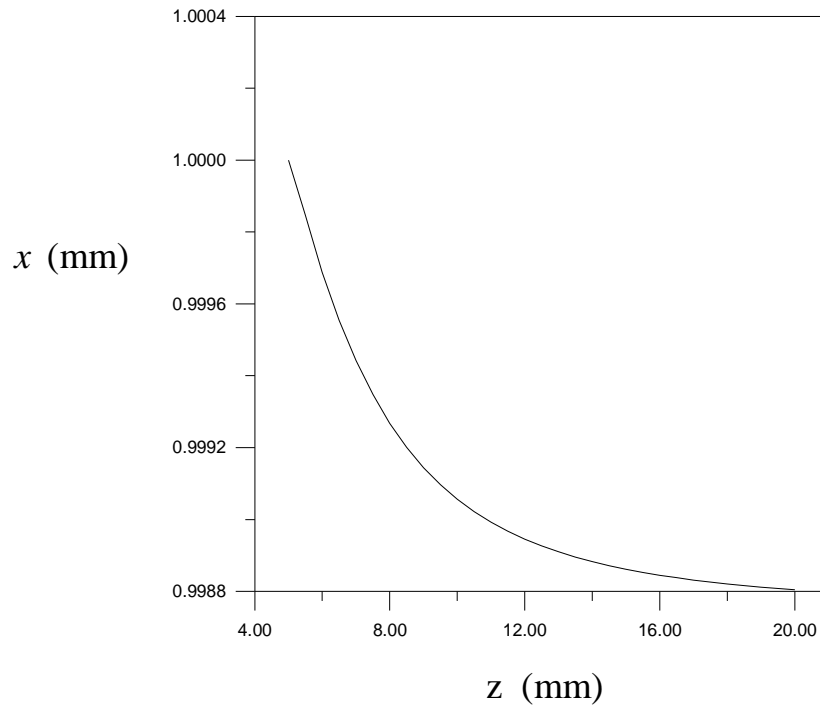
Figure (3-24): The linear magnification of electrostatic quadrupole lens with spherical electrodes in divergence plane as a function of gap angle 2Γ for three values of $b/a = 0.4, 0.425, \text{ and } 0.45$.

3-2-2 The trajectory of charged – particles beam

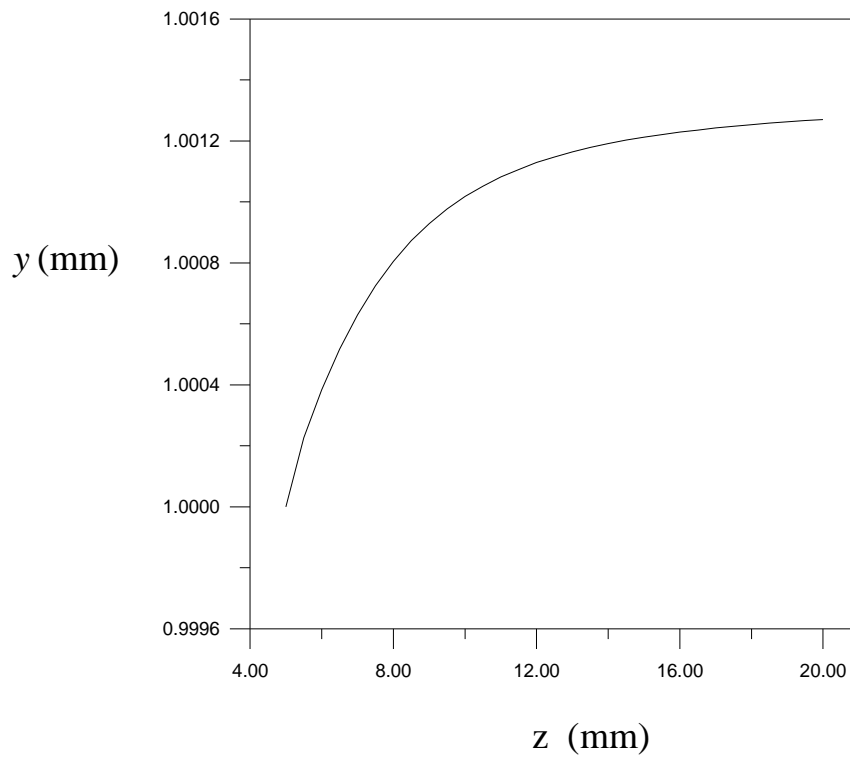
The trajectory of the charged-particles beam traversing the electrostatic quadrupole lens of cylindrical convex differs from these of concave electrodes or spherical electrodes. Under consideration the trajectory has been computed in both x-z and y-z planes under various conditions taking into account the polarity of each electrode which is shown in figure (1-1-a). The trajectory equation of charge- particles which pass through cylindrical convex electrodes has been solved for the modified bell-shaped model by using simplified transformation equations (2-30) and (2-31) which describe the path of charge particles in the convergence and divergence planes to find the trajectory of particle in quadrupole lens and the results are shown in figure (3-4).

In computing the trajectories the initial conditions is given in the case of cylindrical convex electrodes by :

$$x_o = 1 \text{ and } x'_o = 0 ; y_o = 1 \text{ and } y'_o = 0 .$$



Figure(3-4):Trajectories of charge particles beam in electrostatic quadrupole lens of cylindrical convex electrodes for convergence(x-z) plane .

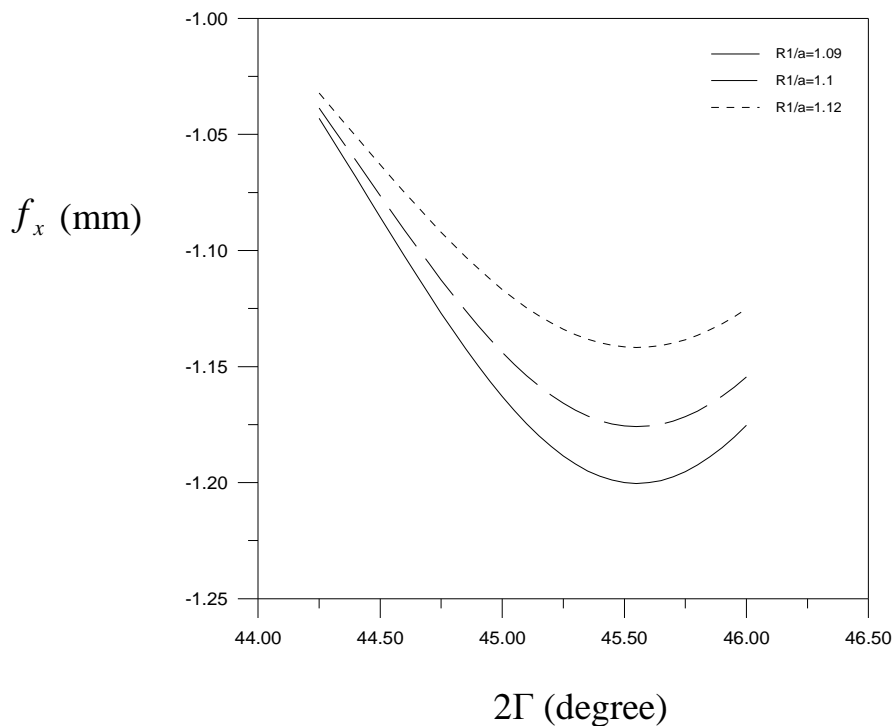


Figure(3-4):Trajectories of charge particles beam in electrostatic quadrupole lens of cylindrical convex electrodes for divergence(y-z) plane .

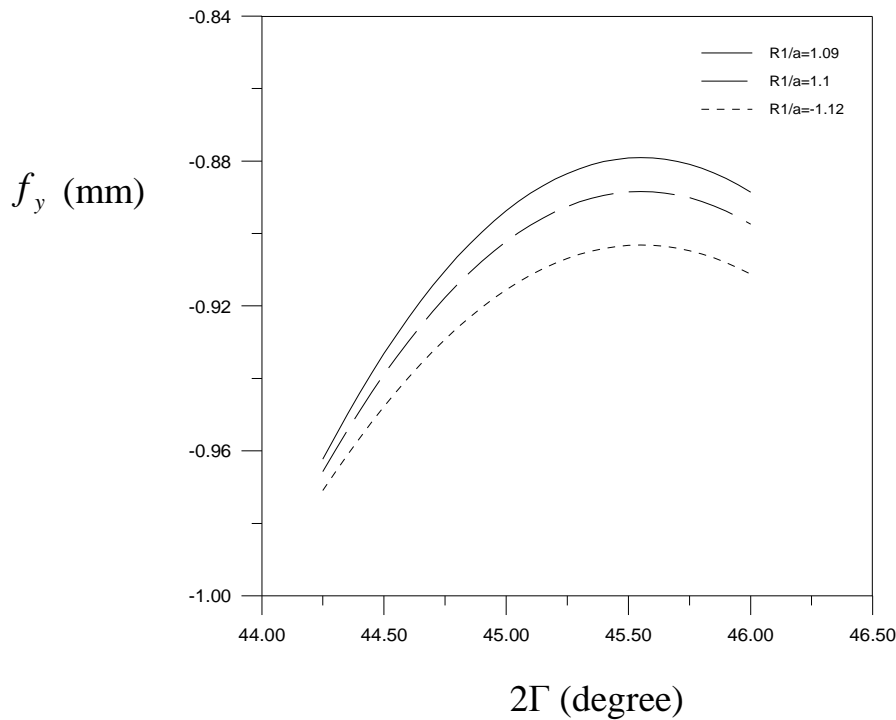
3-2-3 The properties of electrostatic quadrupole lens

3-2-3-1 the focal length and magnification

By using the transfer matrices T_x , T_y which is given in equations (2-30) and (2-31), the first order optical properties such as focal length and magnification have been computed with the aid of equations (2-40) to (2-44) in the convergence and divergence planes. Figures (3-5) and (3-6) show the focal length as a function of 2Γ for three values of $R_1/a = 1.09, 1.1, \text{ and } 1.12$ in both convergence and divergence plane (x and y respectively). The curves of focal length f_x in convergence plane have the same behavior for all values of R_1/a . The focal length f_x which has the negative values decreases with increasing 2Γ and all curves have a minimum values at $2\Gamma = 45.5^\circ$. Also, the ratio $R_1/a = 1.09$ has the lower values of focal length. In the divergence plane the focal length f_y is negative and is increasing with 2Γ increases and each curves of R_1/a have a maximum value at $2\Gamma = 45.5^\circ$.



Figure(3-5): The focal length of convergence plane of electrostatic quadrupole lens with cylindrical convex electrodes as a function of gap angle 2Γ for three values of $R_1/a = 1.09, 1.1, \text{ and } 1.12$.



Figure(3-6): The focal length of divergence plane of electrostatic quadrupole lens with cylindrical convex electrodes as a function of gap angle 2Γ for three values of $R_1/a = 1.09, 1.1, \text{ and } 1.12$.

Figures (3-7) and (3-8) depict the variation of linear magnification with 2Γ for each value of R_1/a in both convergence and divergence planes M_x and M_y , respectively. The positive sign of magnification indicates that the image is erect, and the value of magnification is less than unity indicates that the image is small with respect to the state of the object. In general, the linear magnification in convergence plane M_x has the opposite behavior to the magnification in divergence plane M_y .

The values of M_x are decreasing with 2Γ increases and it has a minimum value at $2\Gamma = 45.5^\circ$ for each curves of R_1/a and all curves increase as 2Γ is increasing beyond this value, but the values of M_y are increasing with 2Γ increases and the values have a maximum value at $2\Gamma = 45.5^\circ$ for each curves of R_1/a .

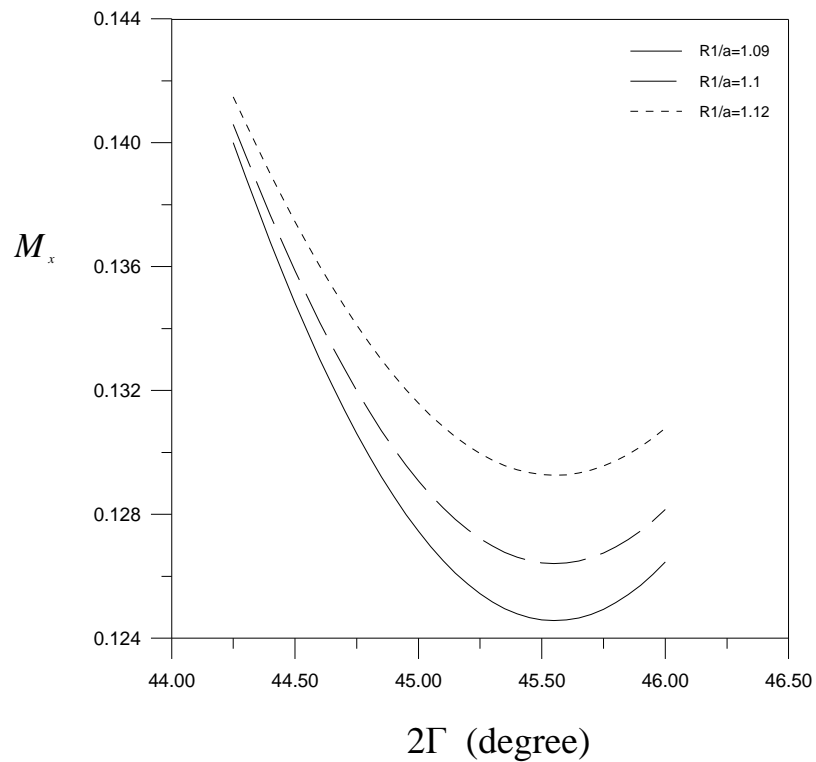


Figure (3-7): The linear magnification of electrostatic quadrupole lens with cylindrical convex electrodes in convergence plane as a function of gap angle 2Γ for three values of $R_1/a = 1.09, 1.1,$ and 1.12 .

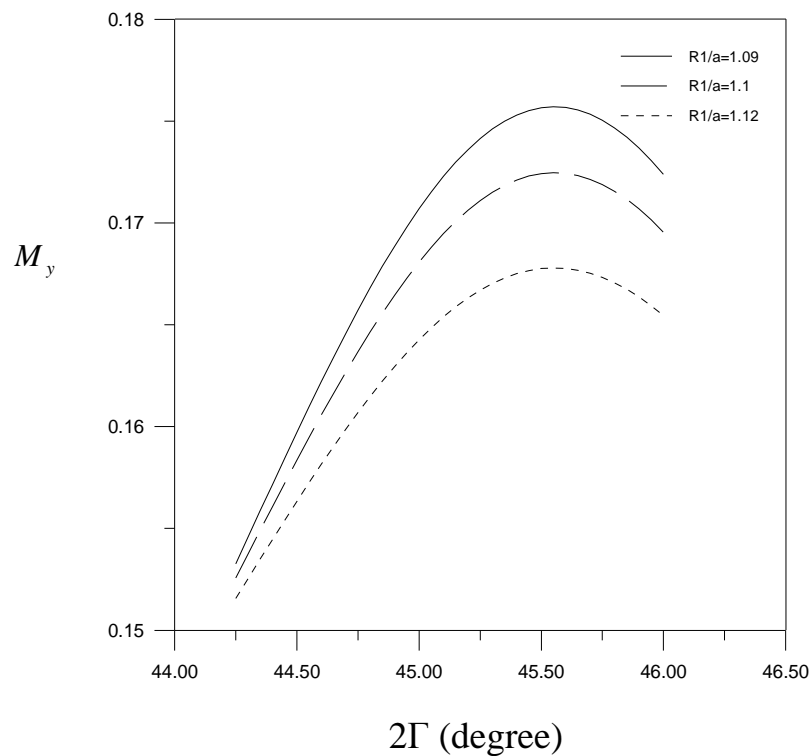
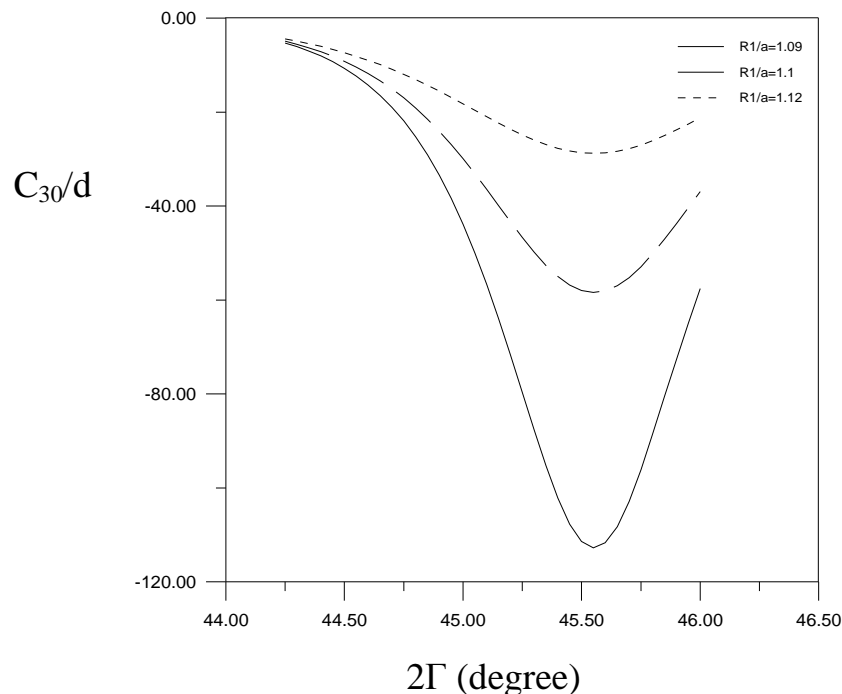


Figure (3-8): The linear magnification of electrostatic quadrupole lens with cylindrical convex electrodes in divergence plane as a function of gap angle 2Γ for three values of $R_1/a = 1.09, 1.1,$ and 1.12 .

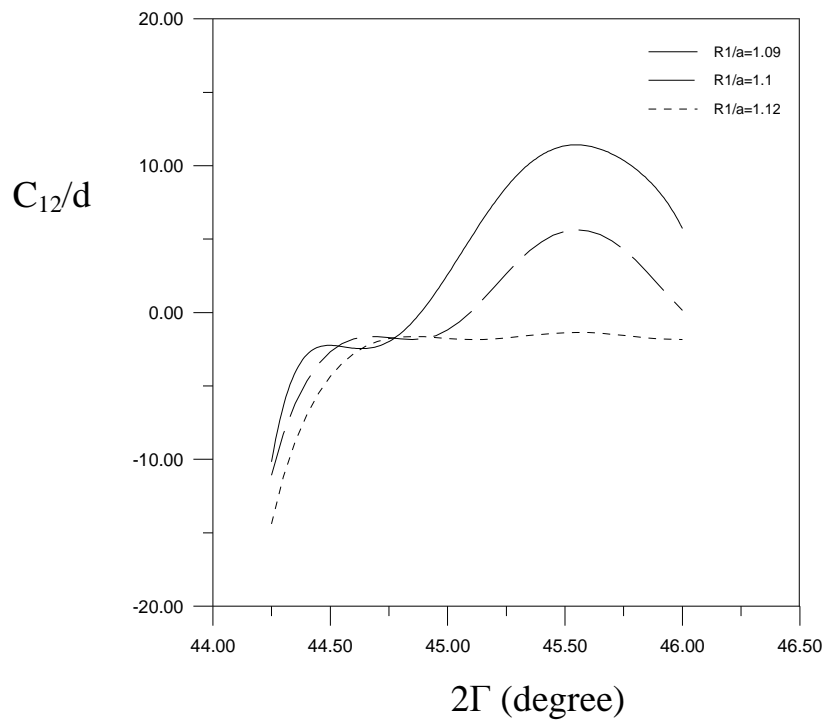
3-2-3-2 the spherical aberration

The spherical and chromatic aberrations have been given considerable attention in the present work since they are the two most important aberration in electron optical systems. The two relative spherical aberration coefficients C_{30}/d and C_{12}/d in the convergence plane of the electrostatic quadrupole lens are shown in figures (3-9) and (3-10) as a function of 2Γ at three values of R_1/a with. The effect of changing the 2Γ and $R_1/a = 1.09, 1.1, \text{ and } 1.12$ are seen clearly on the relative spherical aberration. For C_{30}/d , figure (3-9), it can be seen that for low values of angle 2Γ all curves are coincide and when 2Γ increases the curves are far from each other but have the same behavior, they are decreasing in negative value and have a minimum value at $2\Gamma = 45.5^\circ$. The best minimum value of C_{30}/d at $R_1/a = 1.12$ when the lowest absolute value of spherical aberration coefficient C_{30}/d is found.



Figure(3-9): The relative spherical aberration coefficient C_{30}/d of electrostatic quadrupole lens with cylindrical convex electrodes as a function of gap angle 2Γ for three values of $R_1/a = 1.09, 1.1, \text{ and } 1.12$.

In figure (3-10) the C_{12}/d in low values of angle 2Γ has the same behavior for each value of R_1/a up to an angle $2\Gamma = 44.5^\circ$. All curves overlapping with each other at $2\Gamma = 44.75^\circ$. All curves have a common point of C_{12}/d irrespective to the value of R_1/a and beyond this value the C_{12}/d at R_1/a equal to 1.09 and 1.1 increases in positive with increasing 2Γ , and have a maximum value at $2\Gamma = 44.5^\circ$, but for R_1/a equal to 1.12 and beyond $2\Gamma = 44.55^\circ$ C_{12}/d is stable at negative value. The value of $R_1/a = 1.12$ gives the optimum value of C_{12}/d for most range of 2Γ .

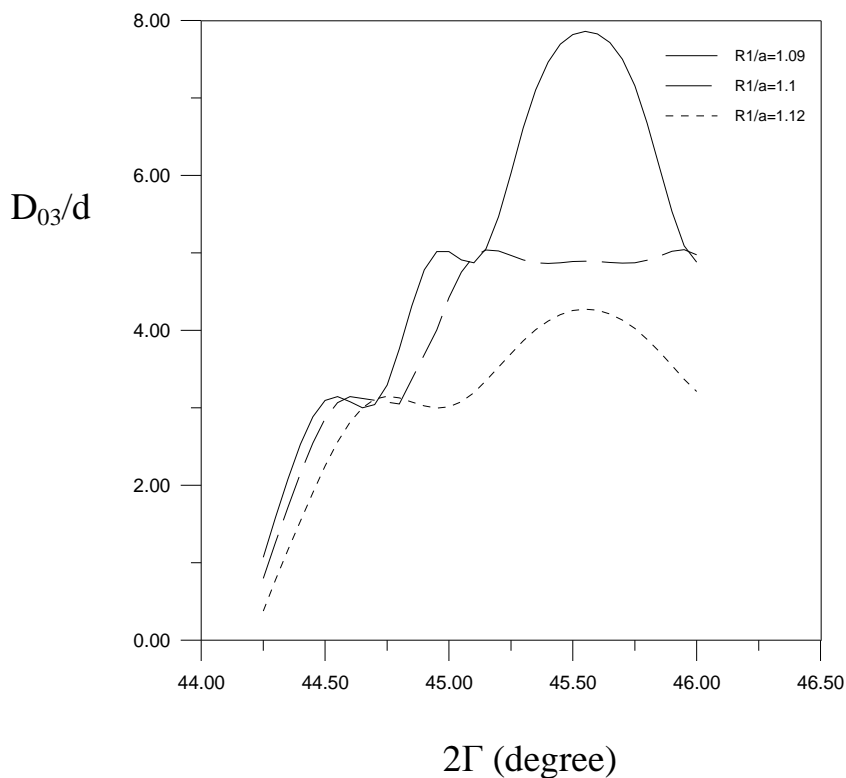


Figure(3-10):The relative spherical aberration coefficient C_{12}/d of electrostatic quadrupole lens with cylindrical convex electrodes as a function of gap angle 2Γ for three values of $R_1/a = 1.09, 1.1,$ and 1.12 .

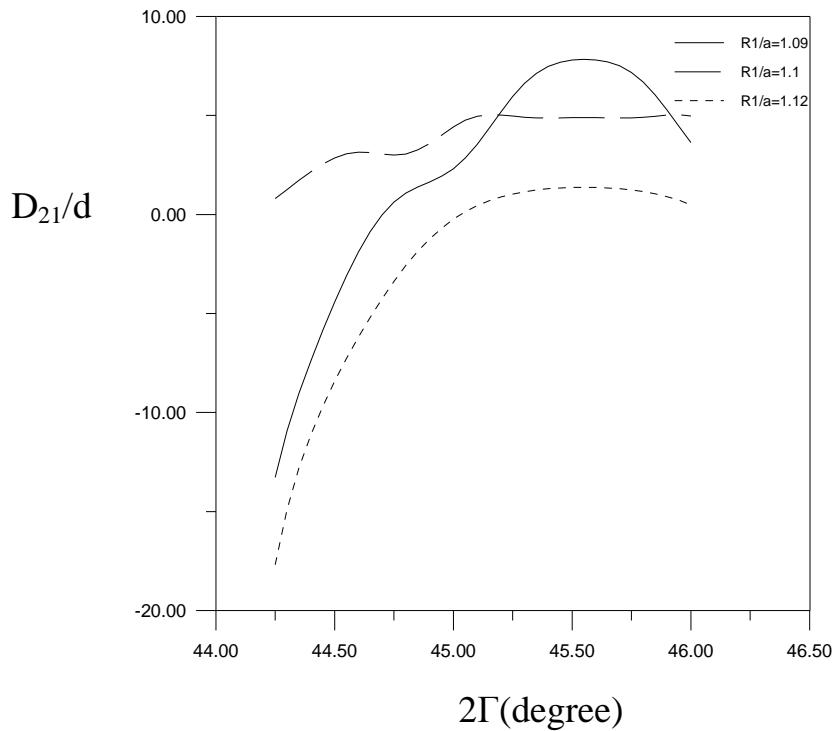
The variation of the two relative spherical aberration coefficients D_{03}/d and D_{21}/d with the angle 2Γ in the divergence plane are shown in figures (3-11) and (3-12). It is seen that the values of D_{03}/d for all values of R_1/a have the same behavior up to $2\Gamma = 44.6^\circ$ as in figure (3-11), then beyond this value of D_{03}/d increases with increasing 2Γ and both curves of $R_1/a = 1.09$ and 1.12 have

a maximum value at $2\Gamma = 45.5^\circ$. But $R_1/a = 1.11$ takes the stable values at range $2\Gamma > 45^\circ$. The best value of R_1/a is (1.12) which gives the best values of spherical aberration coefficient D_{03}/d .

The values of D_{21}/d for each value of R_1/a have the same behavior in low value of 2Γ , these values increase with increasing 2Γ and then for $2\Gamma > 44.75^\circ$ the D_{21}/d of $R_1/a = 1.09$ has a maximum value in positive at $2\Gamma = 45.5^\circ$ and for $R_1/a = 1.1$ the values of D_{21}/d take to stable in positive at $2\Gamma < 45$. For $R_1/a = 1.12$ the D_{21}/d has a maximum value in positive at $2\Gamma = 45.5^\circ$ the last value of R_1/a gives the lowest or the best value of D_{21}/d . The variation of the four relative spherical aberration coefficients as a function of 2Γ for each R_1/a values gives the best values at $R_1/a = 1.12$ for the whole range of 2Γ .



Figure(3-11): The relative spherical aberration coefficient D_{03}/d of electrostatic quadrupole lens with cylindrical convex electrodes as a function of gap angle 2Γ for three values of $R_1/a = 1.09, 1.1,$ and 1.12 .

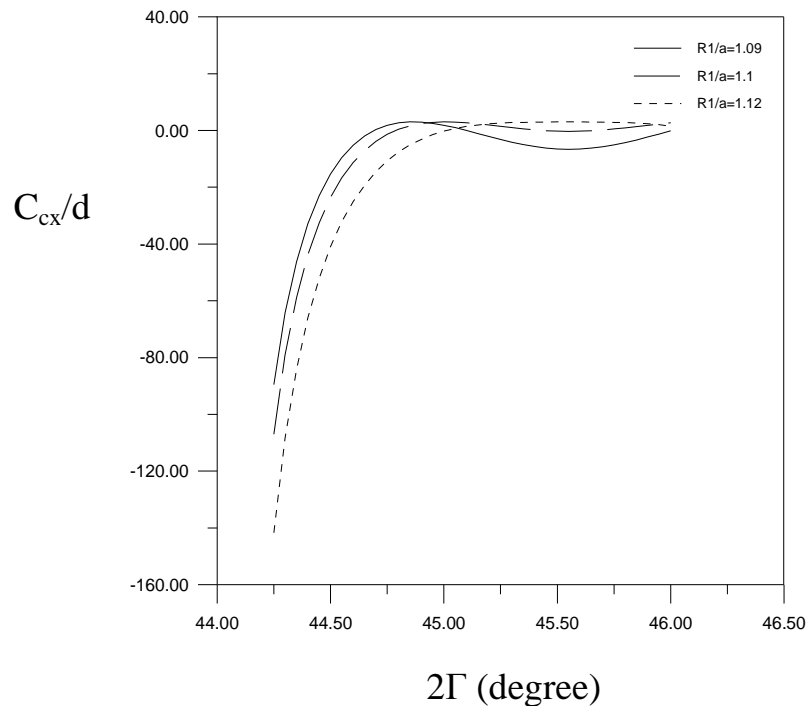


Figure(3-12): The relative spherical aberration coefficient D_{21}/d of electrostatic quadrupole lens with cylindrical convex electrodes as a function of gap angle 2Γ for three values of $R_1/a = 1.09, 1.1,$ and 1.12 .

3-2-3-3 the chromatic aberration

The pair of chromatic aberration coefficients in the convergence plane and the corresponding pair in the divergence plane are plotted in figures (3-13) to (3-16) as a function of the angle 2Γ for three values of $R_1/a = 1.09, 1.1,$ and 1.12 . The coefficients C_{cx}/d in the convergence plane have the same behavior for each values of R_1/a , where C_{cx}/d increases with increasing 2Γ and has the negative values, for $R_1/a = 1.12$ the C_{cx}/d takes a stable values which are less than unity at $2\Gamma \geq 45$, but for $R_1/a = 1.1$ and 1.09 have a minimum value at $2\Gamma = 45.5^\circ$.

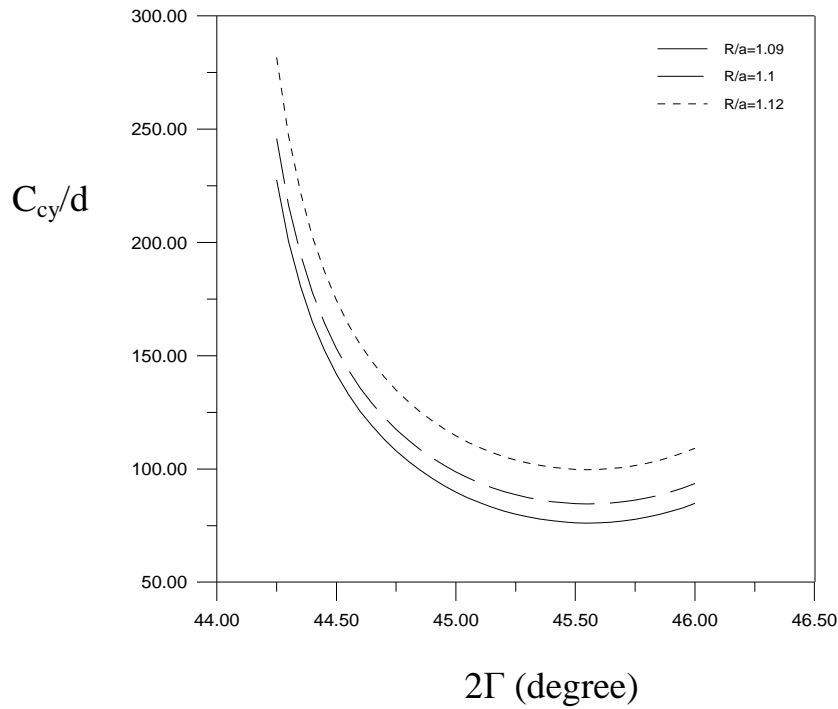
Also, from the figure (3-13) in general the difference between the values is slightly and the best value of chromatic aberration coefficient C_{cx}/d is that for $R_1/a = 1.12$ up to $2\Gamma = 45^\circ$, while R_1/a gives us the best values of chromatic aberration coefficient C_{cx}/d at beyond $2\Gamma > 45^\circ$.



Figure(3-13):The relative chromatic aberration coefficient C_{cx}/d of electrostatic quadrupole lens with cylindrical convex electrodes as a function of gap angle 2Γ for three values of $R_1/a = 1.09, 1.1, \text{ and } 1.12$.

The coefficient C_{cy}/d in the divergence plane has the same behavior for all values of R_1/a as is shown in figure (3-14), where C_{cy}/d decreases with 2Γ increases and all curves have a minimum value at $2\Gamma = 45.5^\circ$. The best value of R_1/a which gives the lowest chromatic aberration coefficient C_{cy}/d is equal to 1.09 for whole range of 2Γ .

Therefore, the designer can use the geometrical dimensions $R_1/a = 1.09$ and $2\Gamma = 45.5^\circ$ to design the electrostatic quadrupole lens which has the best chromatic aberration coefficients in both convergence and divergences planes.



Figure(3-14):The relative chromatic aberration coefficient C_{cy}/d of electrostatic quadrupole lens with cylindrical convex electrodes as a function of gap angle 2Γ for three values of $R_1/a = 1.09, 1.1, \text{ and } 1.12$.

The variation of chromatic aberration coefficient of change of magnification in both convergence and divergence planes C_{mx} and C_{my} and the effect of changing of 2Γ are investigated for three values of $R_1/a = 1.09, 1.1, \text{ and } 1.12$ and the results are shown in figures (3-15) and (3-16). The values of C_{mx} and C_{my} are always positive and have the same behavior, where decrease with increasing 2Γ for low values of angle 2Γ all curves are close to each other at this region. When the angle 2Γ increases the curves are far from each other but all curves have a minimum values at $2\Gamma = 45.5^\circ$ as are shown in figures (3-15) and (3-16).

Also, the $R_1/a = 1.09$ gives the best values of chromatic aberration coefficient of changing of magnification for both convergence and divergence planes for whole range of 2Γ , while the angle $2\Gamma = 45.5^\circ$ gives us the best value of chromatic aberration coefficient of changing magnification.

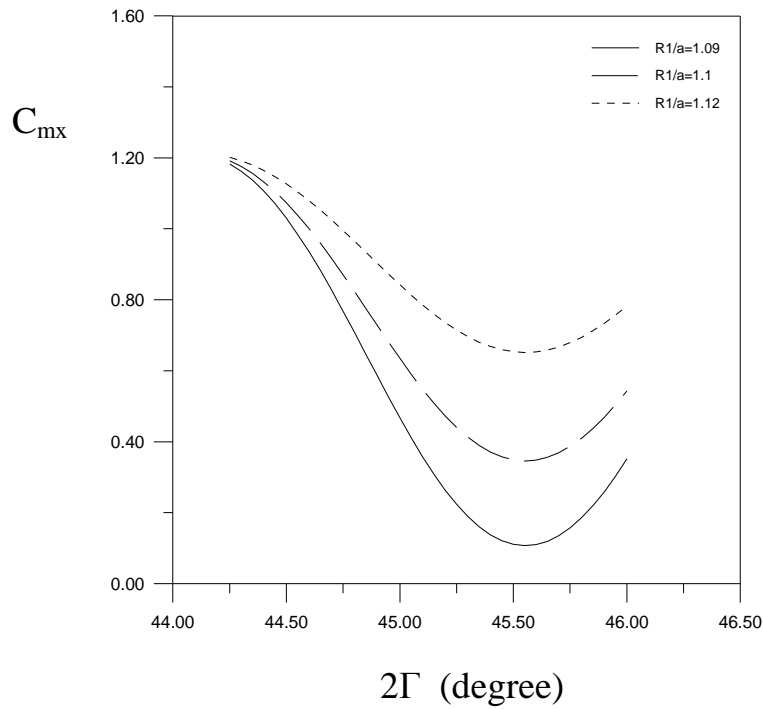
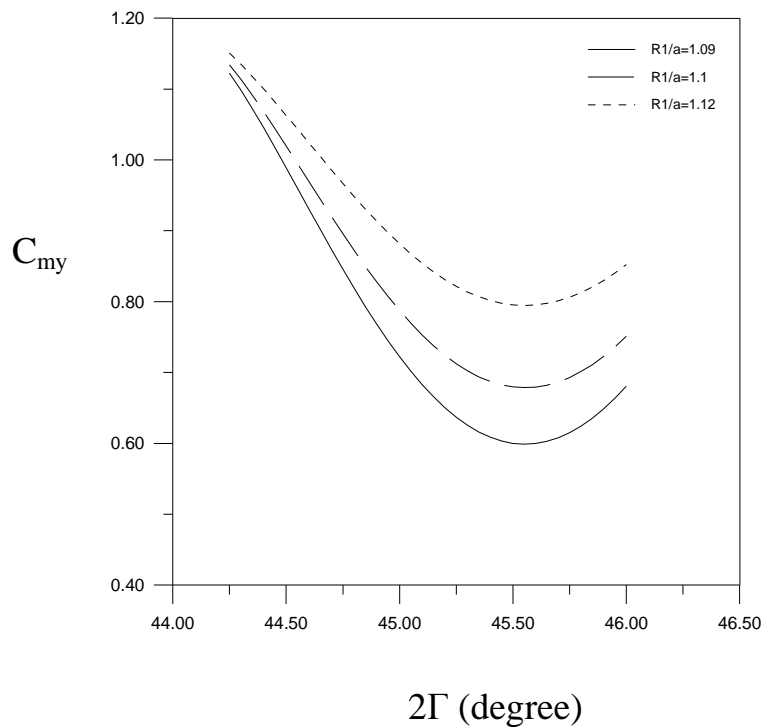


Figure (3-15): The chromatic aberration coefficient of changing magnification C_{mx} for electrostatic quadrupole lens with cylindrical convex electrodes as a function of gap angle 2Γ for three values of $R_1/a = 1.09, 1.1,$ and 1.12 .



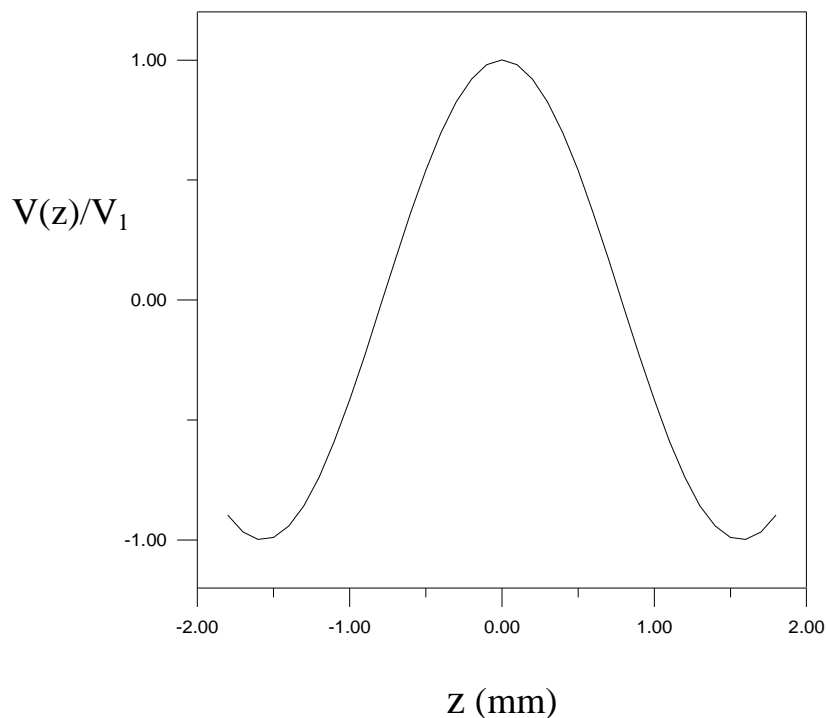
Figure(3-16):The chromatic aberration coefficient of changing magnification C_{my} for electrostatic quadrupole lens with cylindrical convex electrodes as a function of gap angle 2Γ for three values of $R_1/a = 1.09, 1.1,$ and 1.12 .

Finally, it should be mentioned that there is very little published work on the optical properties of the electrostatic quadrupole lens of cylindrical convex electrodes. In the present work the results are very close to that of Kiss et al. [1969] which is the most important of these publications.

3-3 Spherical Electrodes

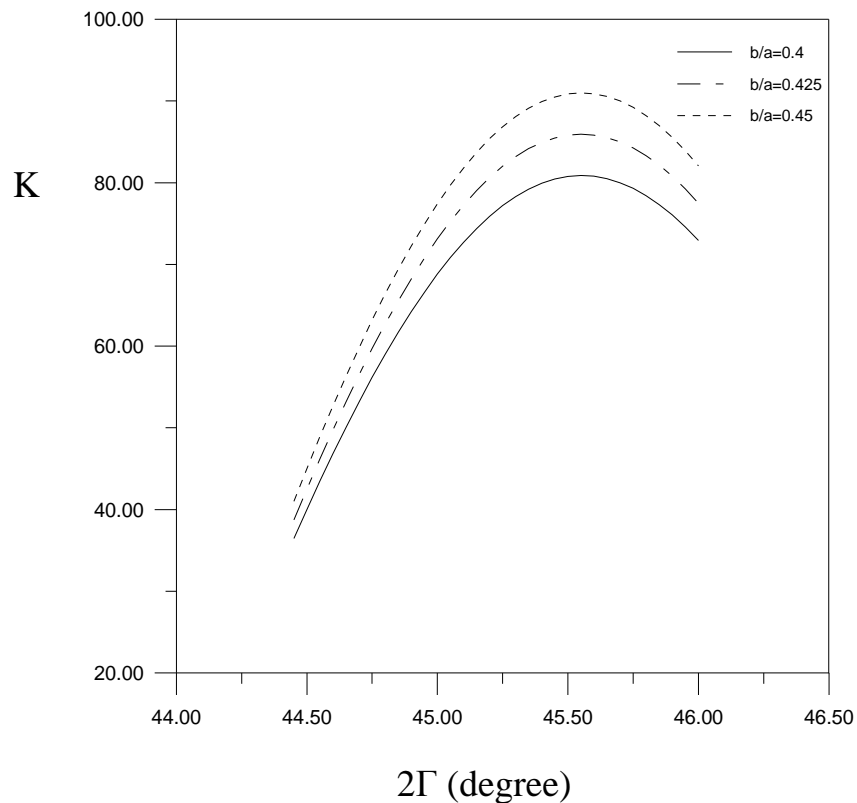
3-3-1 The potential distribution

In this part of present work the four spheres electrodes of small radius relative to the aperture a as shown in figure (2-4) have been used studied. The potential distribution of quadrupole lens with spherical electrodes is calculated by equation (2-9). The result shows that the bell-shaped field model is very close approximation to the potential distribution of quadrupole lens as in figure (3-17). This result is in agreement with the results mentioned in various references (see for example Kiss et al. 1970).



Figure(3-17): The potential distribution ratio of electrostatic quadrupole lens of spherical electrodes which is very close to bell-shaped field mode.

Figures (3-18) and (3-19) show the coefficients K and β as a function of 2Γ at various value of electrodes radius to aperture radius ratio b/a , these parameters are calculated from equations (2-20) and (2-23) respectively. From the calculations, all curves have the same behavior for each values of b/a . The values of K and β increase with increasing 2Γ at constant b/a and with increasing b/a at constant 2Γ . For all values of b/a the values of K and β have maximum value at $2\Gamma = 45.55^\circ$.



Figure(3-18): The coefficient of electrode shape K for electrostatic quadrupole lens with spherical electrodes as a function of gap angle 2Γ for three values of $b/a = 0.4, 0.425$ and 0.45 .

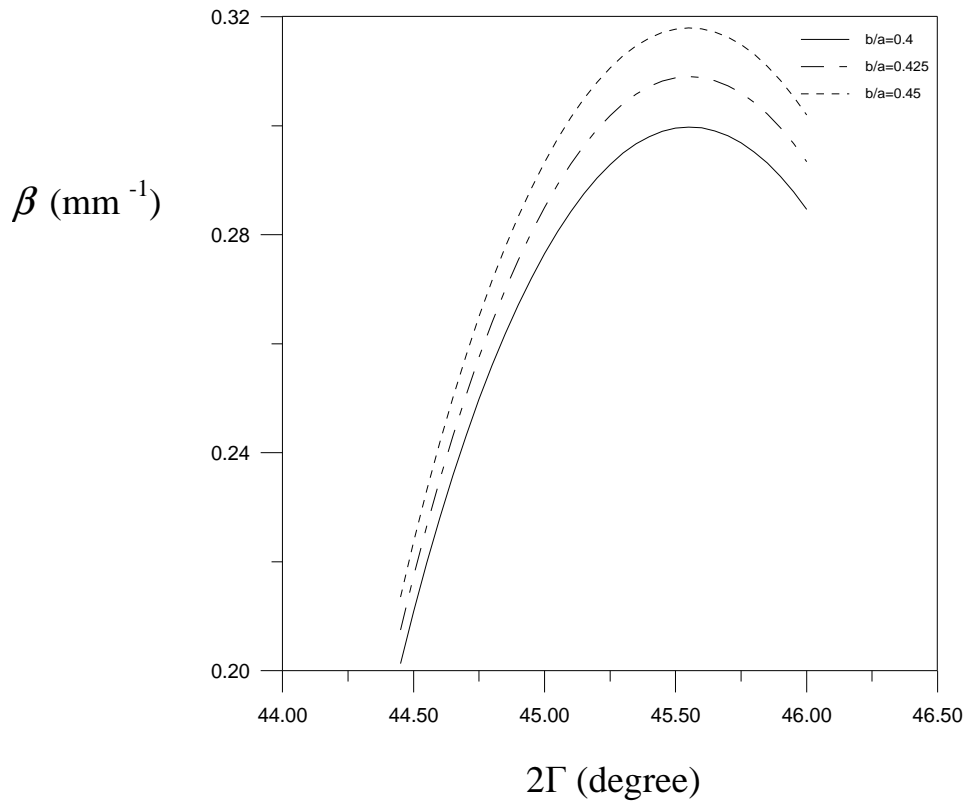


Figure (3-19): The excitation parameter β (mm^{-1}) for electrostatic quadrupole lens with spherical electrodes as a function of gap angle 2Γ for three values of $b/a = 0.4, 0.425$ and 0.45 .

3-3-2 The trajectory of charged – particles beam

The figure (3-20) shows the trajectory of charged particles which passes through electrostatic quadrupole lens with spherical electrodes. The trajectory equation of charge particles has been solved for the bell-shaped model by using simplified transformation. The charged particles suffer from the effect of convergence plane xOz will deflected toward the optical axis, but these are suffer from the effect of divergence plane yOz will deflected away from the optical axis.

The initial condition of the trajectory have been given :

$$x_o = 1 \quad \text{and} \quad x'_o = 0 ; \quad y_o = 1 \quad \text{and} \quad y'_o = 0 .$$

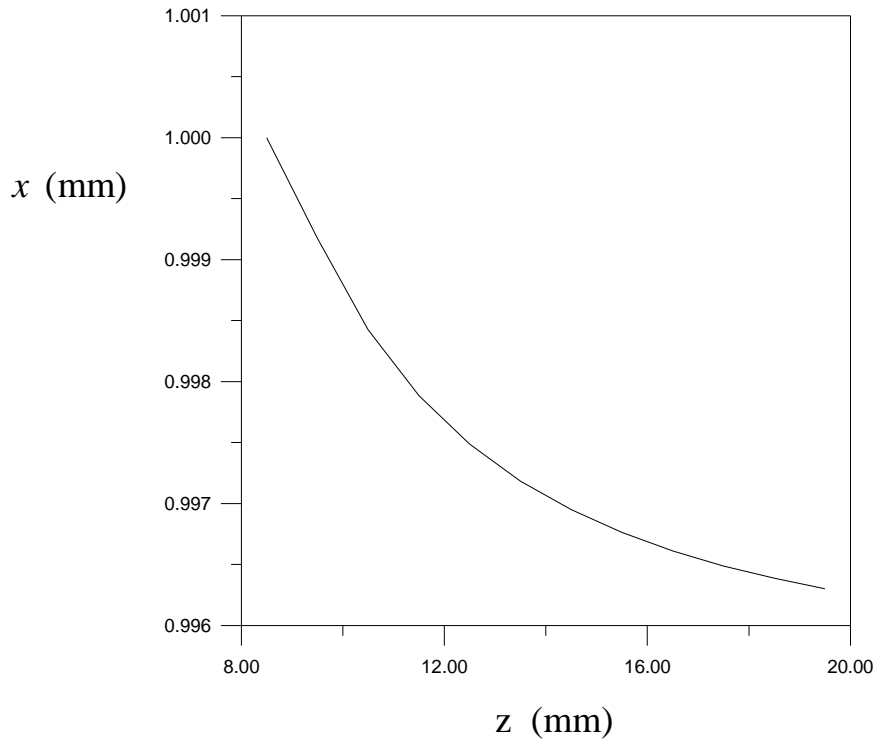


Figure (3-20): Trajectories of charge particles beam in electrostatic quadrupole lens of spherical electrodes for convergence(x - z) plane .

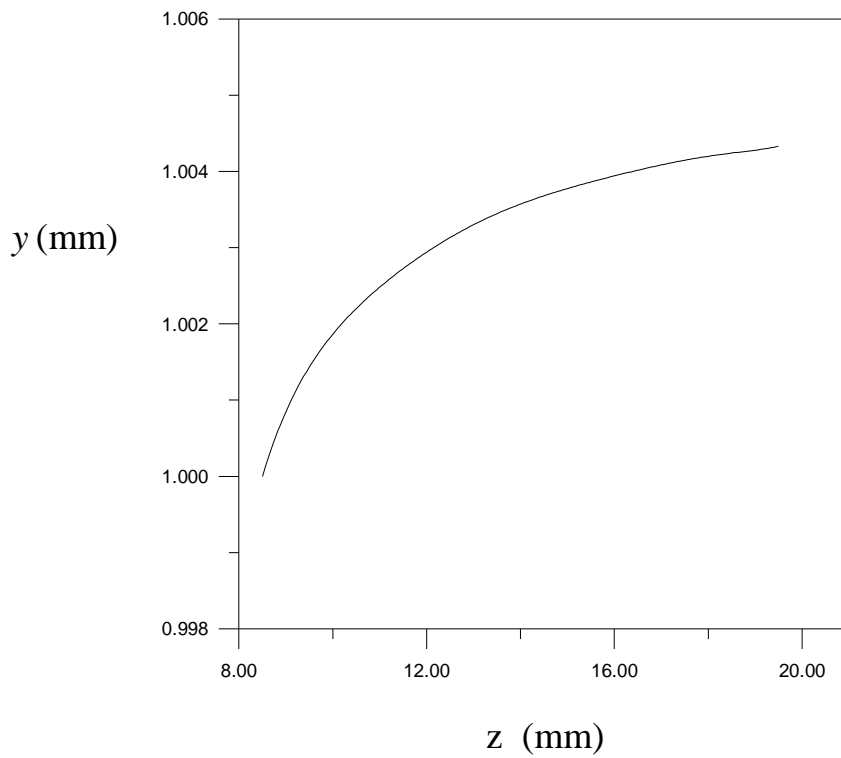


Figure (3-20): Trajectories of charge particles beam in electrostatic quadrupole lens of spherical electrodes for divergence (y - z) plane.

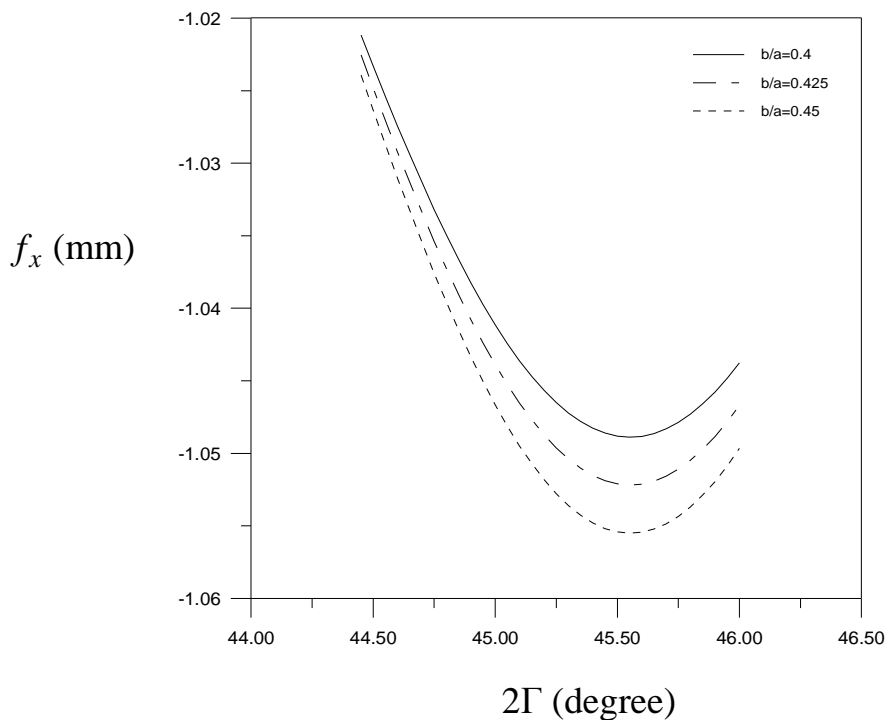
3-3-3 The properties of electrostatic quadrupole lens

3-3-3-1 the focal length and magnification

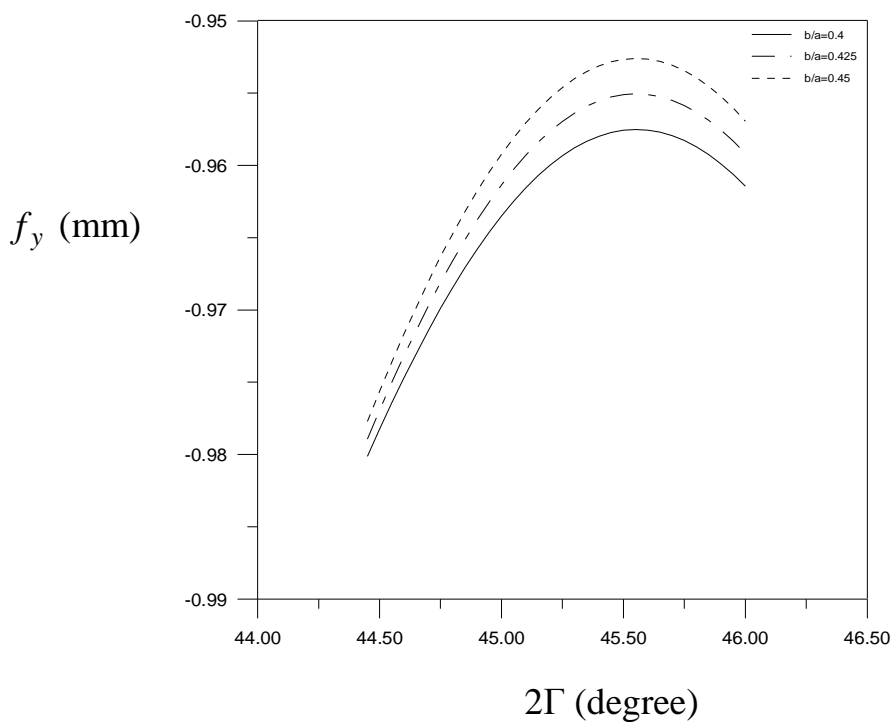
The effect of varying the b/a of the electrostatic quadrupole lens with spherical electrode, and the gap angle between the electrodes 2Γ on the properties of the electrostatic quadrupole lens has been investigated. The value of b/a is varied in the interval $0.124 \leq b/a \leq 0.5$, and hence the value of 2Γ is varied in the interval $44.3 \leq 2\Gamma \leq 46.00$.

The computed focal lengths for different b/a as the function of the gap angle 2Γ , in both convergence and divergence planes are shown in figures (3-21) and (3-22) respectively. In convergence plane f_x is negative and the values decreases with 2Γ increases at constant value of b/a and decreases with b/a increase at constant 2Γ .

Therefore, for all values of b/a the f_x have minimum value at $2\Gamma = 45.5^\circ$. In divergence plane f_y is negative and the values increase with increasing 2Γ for all value of b/a . Therefore, at 2Γ is equal to 45.5° all curve of b/a have maximum value at $2\Gamma = 45.5^\circ$.



Figure(3-21): The focal length of convergence plane for electrostatic quadrupole lens with spherical electrodes as a function of gap angle 2Γ for three values of $b/a = 0.4, 0.425, \text{ and } 0.45$.



Figure(3-22): The focal length of divergence plane of electrostatic quadrupole lens with spherical electrodes as a function of gap angle 2Γ for three values of $b/a = 0.4, 0.425, \text{ and } 0.45$.

Figures (3-23) and (3-24) show the effect of changing the gap angle 2Γ and electrode radius to aperture radius ratio b/a on the magnification in both convergence M_x and divergence planes M_y , respectively. The values of M_x and M_y are always positive and less than unity. From figure (3-23) the M_x decreases with increasing 2Γ for all values of b/a and it has a minimum value for all value of b/a at $2\Gamma = 45.5^\circ$. In figure (3-24) the M_y increases with increasing 2Γ up to $2\Gamma = 45.5^\circ$ where it has a maximum value for all values of b/a . It can be concluded that the quadrupole lens forms a line image of the point object. Therefore, astigmatic image is always formed by the single quadrupole lens.

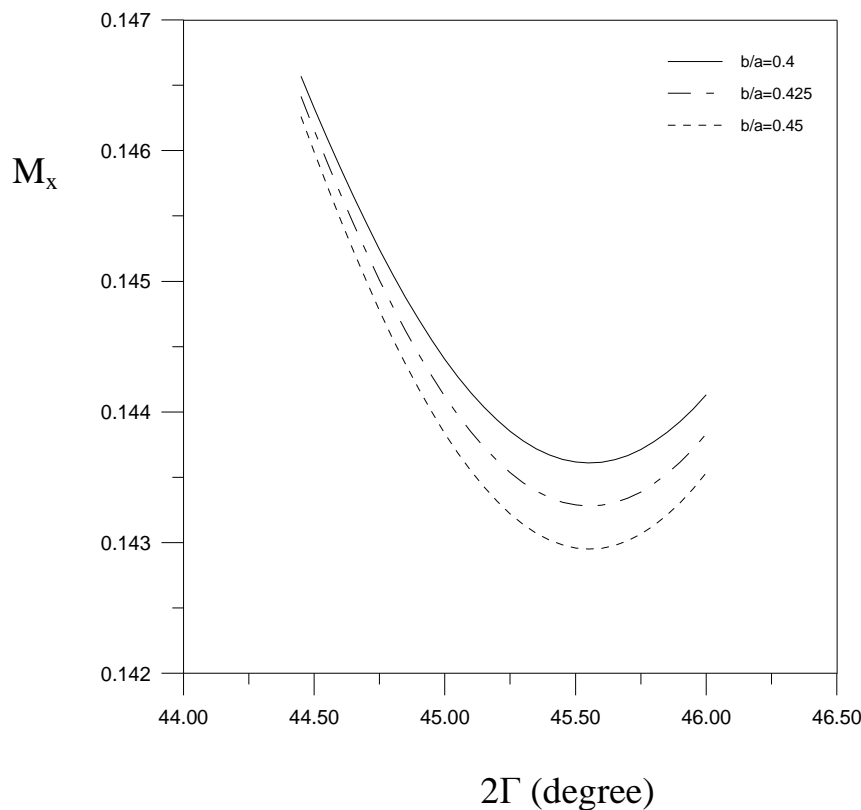
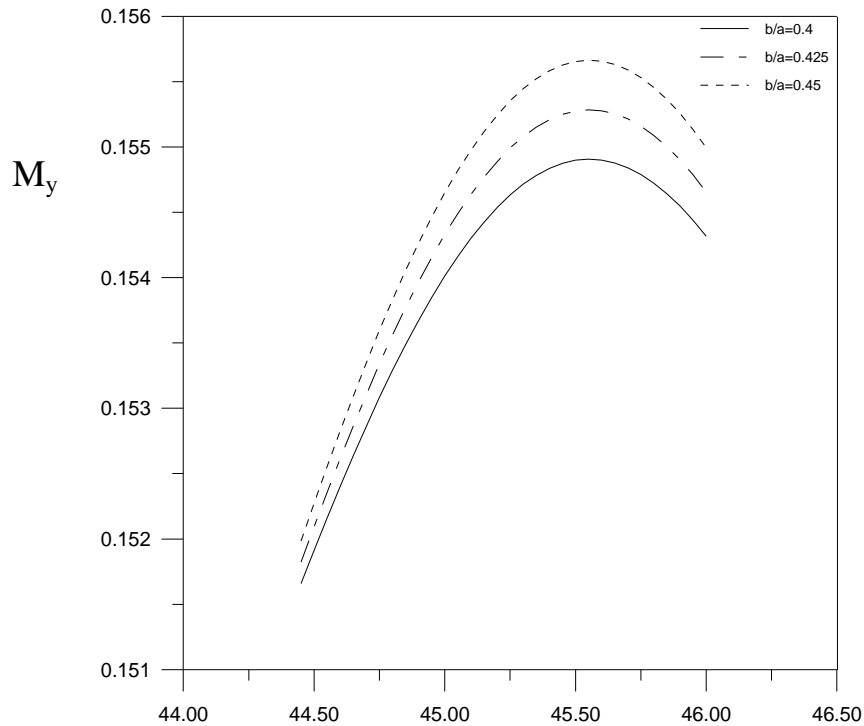


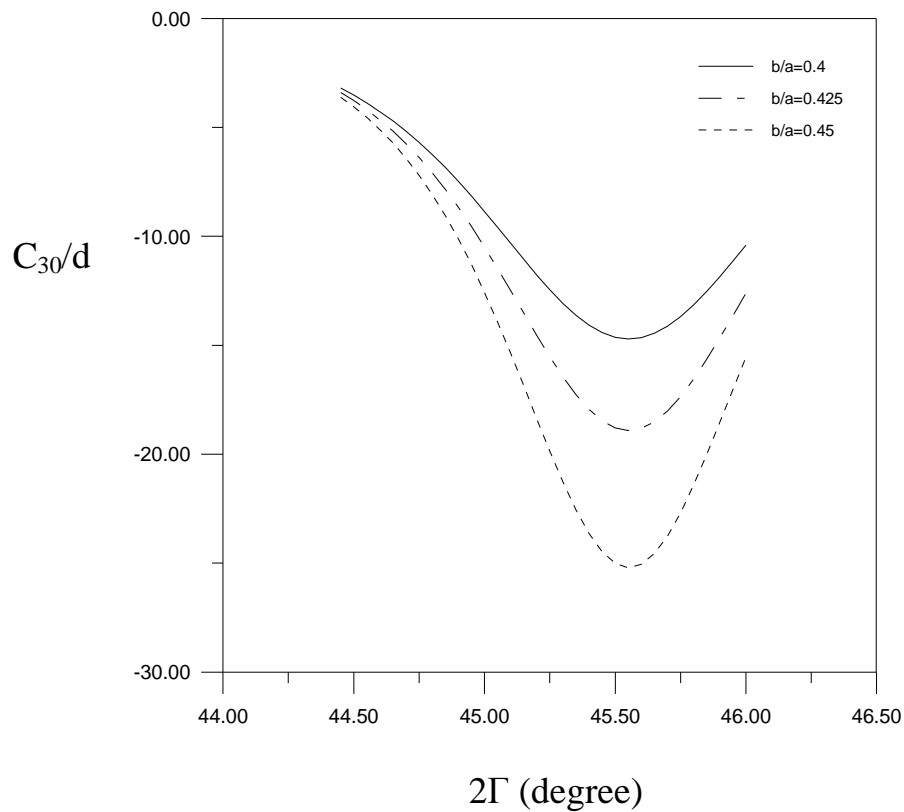
Figure (3-23): The linear magnification of electrostatic quadrupole lens with spherical electrodes in convergence plane as a function of gap angle 2Γ for three values of $b/a = 0.4, 0.425, \text{ and } 0.45$.



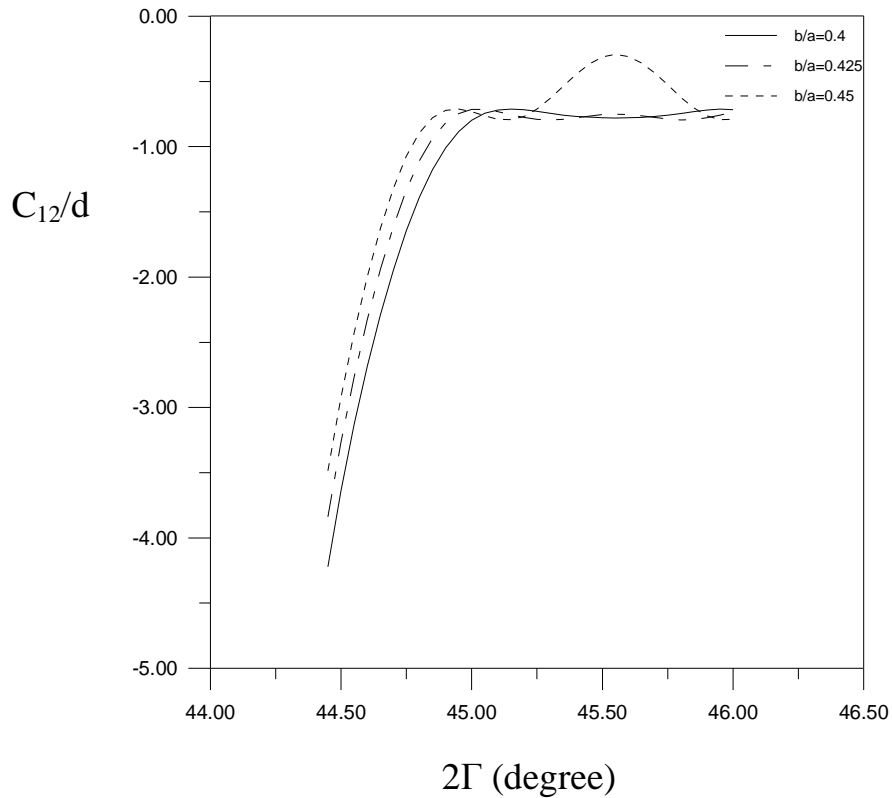
3-3-3-2 the spherical aberration

The relative spherical aberration coefficients as a function of 2Γ for three values of b/a in the convergence plane C_{30}/d and C_{12}/d , and in the divergence plane D_{03}/d and D_{21}/d are shown in figures (3-25) to (3-28). From figure (3-25) the values of C_{30}/d is negative, and the value of C_{30}/d decreases with 2Γ increases up to $2\Gamma = 45.6^\circ$ and for all values of b/a the C_{30}/d have minimum value at $2\Gamma = 45.6^\circ$. Also, when the values of ratio b/a increase the coefficient C_{30}/d is decreasing.

The value of C_{12}/d as in figure (3-26) is always negative and increases with increasing 2Γ until $2\Gamma = 45^\circ$ for all value of b/a , but at $2\Gamma > 45^\circ$ the C_{12}/d has a stable values with increasing 2Γ for $b/a = 0.4$ and 0.425 . But for $b/a = 0.45$ the C_{12}/d has maximum value at $2\Gamma = 45.5^\circ$. The ratio $b/a = 0.4$ give us the best values of C_{12}/d for whole range of 2Γ .



Figure(3-25): The relative spherical aberration coefficient C_{30}/d of electrostatic quadrupole lens with spherical electrodes as a function of gap angle 2Γ for three values of $b/a = 0.4, 0.425, \text{ and } 0.45$.



Figure(3-26): The relative spherical aberration coefficient C_{12}/d of electrostatic quadrupole lens with spherical electrodes as a function of gap angle 2Γ for three values of $b/a = 0.4, 0.425, \text{ and } 0.45$.

Figure (3-27) shows the value of D_{03}/d has the same behavior for all values of b/a and it's always positive and increases with increasing 2Γ . The ratio $b/a = 0.4$ give us the best values of D_{03}/d in whole range of 2Γ . The last parameter of spherical aberration coefficients is D_{21}/d as shown in figure (3-28). The value of D_{21}/d is always negative, and the values increases with 2Γ increases. For $b/a = 0.4$ the D_{21}/d takes to stable values at $2\Gamma \geq 45$.

One can be concluded from figures (3-25) to (3-28) that the ratio of electrode radius to aperture radius $b/a = 0.4$ is favorable as far as the relative spherical aberration coefficients. This result is very close with the results mentioned in various references (see for example Kiss et al. 1970).

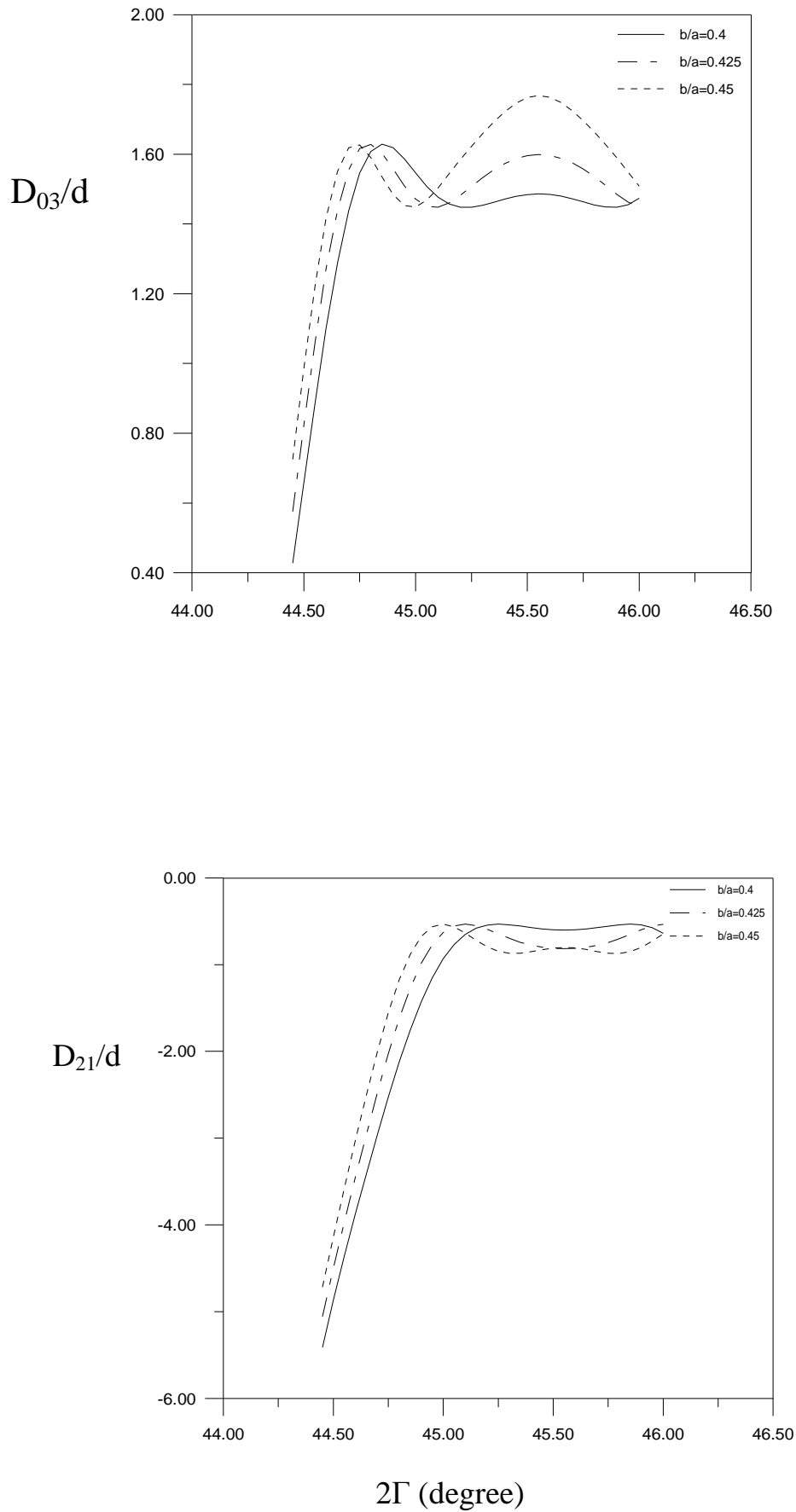
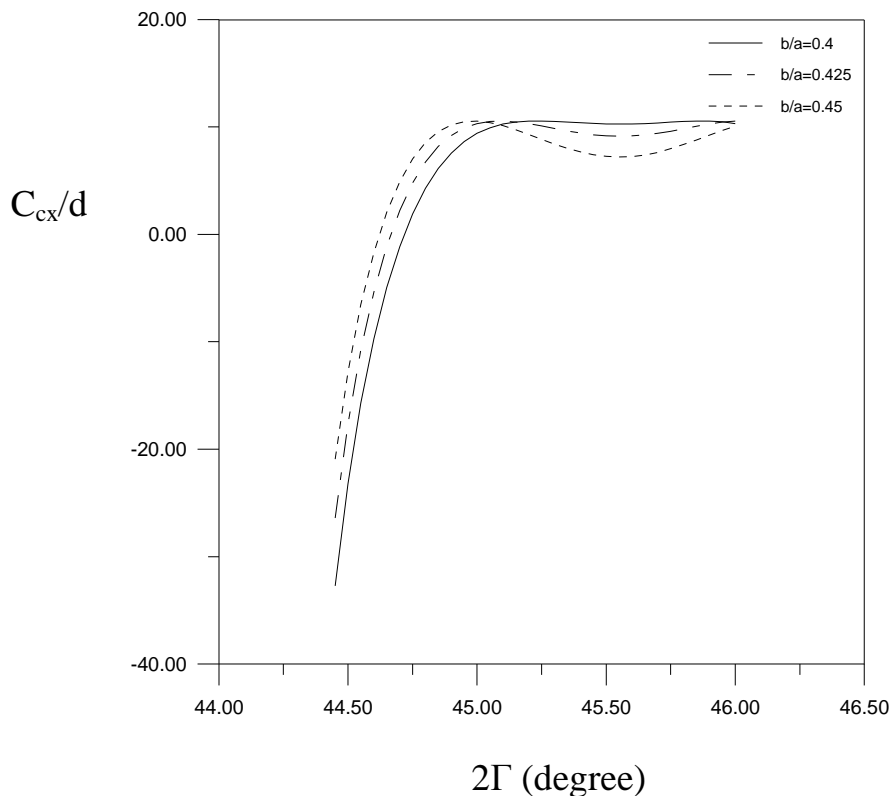


Figure (3-28): The relative spherical aberration coefficient D_{21}/d of electrostatic quadrupole lens with spherical electrodes as a function of gap angle 2Γ for three values of $b/a = 0.4, 0.425, \text{ and } 0.45$.

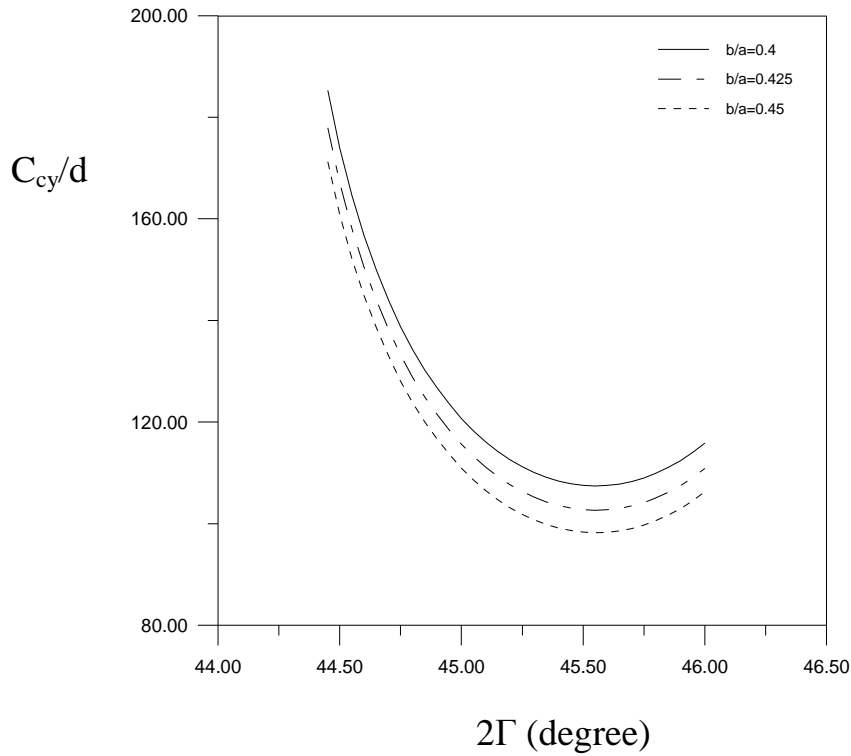
3-3-3-3 the chromatic aberration

The relative chromatic aberration coefficients as a function of 2Γ for three values of $b/a = 0.4, 0.425, \text{ and } 0.45$ are shown in figures (3-29) to (3-32). From the figure (3-29) C_{cx}/d in convergence plane has the same behavior for all values of b/a in wide range $44.4^\circ \leq 2\Gamma \leq 45.00^\circ$. The value of C_{cx}/d for $b/a = 0.4$ takes to stable values at $2\Gamma \geq 45^\circ$. Zero value of C_{cx}/d is found at $2\Gamma = 44.65^\circ, 44.6^\circ, \text{ and } 44.55^\circ$, for $b/a = 0.4, 0.425 \text{ and } 0.45$ respectively as are shown in figure (3-29).

From figure (3-30) the C_{cy}/d in divergence plane is always positive and decreases with 2Γ increases for all values of b/a . The minimum value of C_{cy}/d is happening at $2\Gamma = 45.5^\circ$ for all values of b/a .

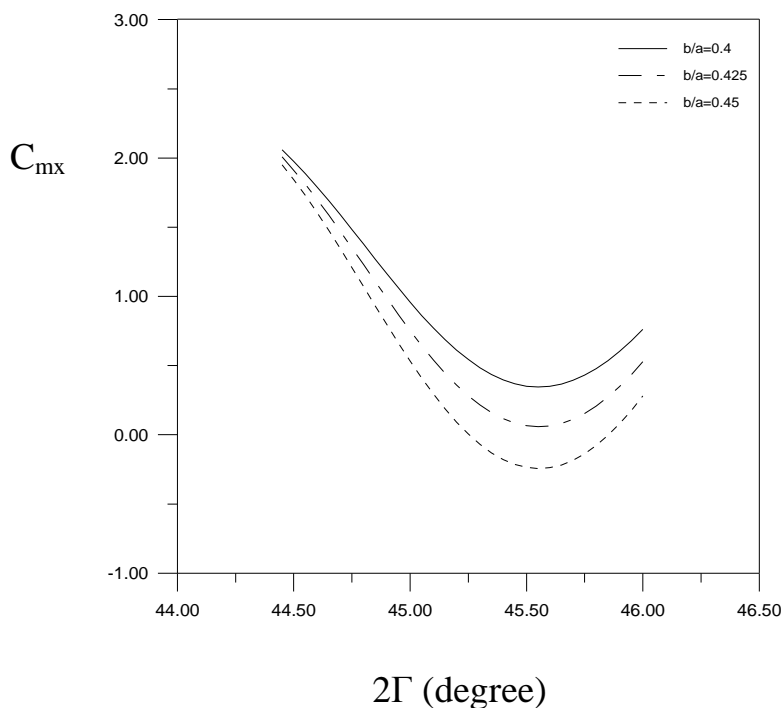


Figure(3-29):The relative chromatic aberration coefficient C_{cx}/d of electrostatic quadrupole lens with spherical electrodes as a function of gap angle 2Γ for three values of $b/a = 0.4, 0.425, \text{ and } 0.45$.

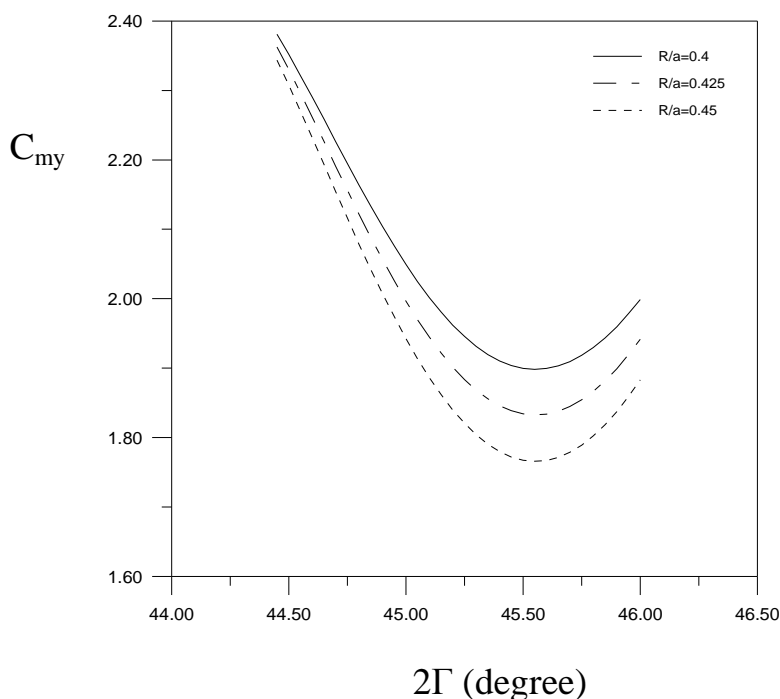


Figure(3-30):The relative chromatic aberration coefficient C_{cy}/d of electrostatic quadrupole lens with spherical electrodes as a function of gap angle 2Γ for three values of $b/a = 0.4, 0.425, \text{ and } 0.45$.

The chromatic aberration coefficient of changing of magnification in both convergence and divergence planes C_{mx} and C_{my} and the effect of changing 2Γ are computed for three values of $b/a = 0.4, 0.425, 0.45$. The variation of C_{mx} is shown in figure (3-31) and this coefficient has the same behavior for all values of $b/a = 0.4, 0.425, 0.45$, where it decreases with increasing 2Γ for all values of b/a . It is always positive for $b/a = 0.4$ and 0.425 and the minimum values of C_{mx} are positive at $2\Gamma = 45.5^\circ$, but for $b/a = 0.45$ is positive and negative and the minimum value of C_{mx} is negative at $2\Gamma = 45.5^\circ$. Figure (3-32) shows the C_{my} is always positive and decreases with 2Γ increases for all values of b/a and the minimum values of C_{my} curve at $2\Gamma = 45.5^\circ$.



Figure(3-31): The chromatic aberration coefficient C_{mx} (mm) of changing of magnification for electrostatic quadrupole lens with spherical electrodes as a function of gap angle 2Γ for three values of $b/a = 0.4, 0.425,$ and 0.45 .



Figure(3-32): The chromatic aberration coefficient C_{my} (mm) of changing of magnification for electrostatic quadrupole lens with spherical electrodes as a function of gap angle 2Γ for three values of $b/a = 0.4, 0.425,$ and 0.45 .

4. CONCLUSIONS AND RECOMMENDATIONS FOR FUTURE WORK

4-1 Conclusions

It appears from the present investigation that it various types of electrostatic quadrupole lenses can be designed different from hyperbolic electrodes shape with better properties such as cylindrical convex and spherical electrodes. The quadrupole lens system has many variable geometrical and operational parameters; thus conclusive result is rather difficult. However, from the present investigation one may conclude the following:

(a) It appears from the suggested designs of cylindrical convex electrodes of electrostatic quadrupole lens that the most favorable field model which is very close to the shape of the axial potential distribution for each design like; the modified bell-shaped model for cylindrical convex electrodes and the bell-shaped model for spherical electrodes. This field model gives the best optical properties for each design of electrodes shape.

(b) The present work shows that the electrostatic quadrupole lens of cylindrical convex electrodes gives the best optical properties at optimum angular distance $2\Gamma = 45.5^\circ$ and $R_1/a = 1.09$, but at $R_1/a = 1.12$ it gives the spherical aberration coefficients better than at $R_1/a = 1.09$.

(c) The electrostatic quadrupole lens of spherical electrodes gives the best optical properties at optimum $2\Gamma = 45.5^\circ$ and $b/a = 0.4$, but at $b/a = 0.45$ it gives the chromatic aberration coefficients best than at $b/a = 0.4$.

(d) In general, the electrostatic quadrupole lens of spherical electrodes gives the best result of aberration parameter C_{cy} and all spherical aberration parameters than the electrostatic quadrupole lens of cylindrical convex electrodes. But the electrostatic quadrupole lens of cylindrical convex electrodes gives the better values of C_{cx} , C_{mx} and C_{my} than spherical electrodes.

4-2 Recommendations For Future Work

The following topics may be recommended for future work:

- (a) Study the effect of other types of field distribution on the properties of electrostatic quadrupole lens for each design.
- (b) Study the effect of other types of an electrode shape such as polygonal or plane electrodes on the field distribution and on the properties of electrostatic quadrupole lens.
- (c) Study the design and properties of an electrostatic quadrupole lens with different electrode shape when the effect of the relativistic velocities of the charged particles is taken into account.
- (d) The optical properties of quadrupole lens can be studied with the combined electrostatic and magnetic lens or with magnetic lens only for each design of quadrupole lens.

<i>Abstract</i>	iv
<i>List of Symbols</i>	viii
1- INTRODUCTION	
1-1 Electrostatic Quadrupole Lens	1
1-2 Quadrupole Lenses Applications	4
1-3 Historical Development	7
1-4 Aim Of The Project	11
2- PROPERTIES OF ELECTROSTATIC QUADRUPOLE LENS FOR DIFFERENT ELECTRODE SHAPE	
2-1 The Electrode Shape of Quadrupole Lens	12
2-2 Field Models For Quadrupole Lenses	13
2-3 Quadrupole Field In Cylindrical Convex Electrodes	15
2-4 Quadrupole Field In Spherical Electrodes	19
2-5 First–Order Optical Properties For An Electrostatic Quadrupole Lens	20
2-5-1 The equation of motion	20
2-5-2 The focal lengths	24
2-5-3 The magnification	25
2-6 Lens Aberrations	26
2-6-1 Spherical aberration of a quadrupole lens	27
2-6-2 Chromatic aberration	29
2-7 Computer program for computing the beam trajectory, the optical properties and the aberration coefficients of electrostatic quadrupole lens	31
3- RESULTS AND DISCUSSION	
3-1 Introduction	33
3-2 Cylindrical Convex Electrodes	33

3-2-1 The potential distribution	33
3-2-2 The trajectory of beam charged–particles	36
3-2-3 The properties of electrostatic quadrupole lens	38
3-2-3-1 the focal length and magnification	38
3-2-3-2 the spherical aberration	41
3-2-3-3 the chromatic aberration	44
3-4 Spherical Electrodes	48
3-4-1 The potential distribution	48
3-4-2 The trajectory of beam charged – particles	50
3-4-3 The properties of electrostatic quadrupole lens	52
3-4-3-1 the focal length and magnification	52
3-4-3-2 the spherical aberration	55
3-4-3-3 the chromatic aberration	59
4- CONCLUSIONS AND RECOMMENDATIONS FOR FUTURE WORK	
4-1 Conclusions	62
4-2 Recommendations For Future Work	63
References	64

Examination Committee Certification

We certify that we have read the thesis entitled “**Determination of the Most Favorable Shapes for the Electrostatic Quadrupole Lens**”, and as an examination committee, examined the student “**Sura Allawi Obaid Al-Zubaidy**” on its contents, and that in our opinion it is adequate for the partial fulfillment of the requirements for the degree of **Master of Science in Physics**.

Signature:

Name: Dr. Ayad A. Al-Ani

Title: (Chairman)

Date: / 4 / 2007

Signature:

Name: Dr. Shatha M. Al-Hilly

Title: (Member)

Date: / 4 / 2007

Signature:

Name: Dr. Adawiya J. Haider

Title: (Member)

Date: / 4 / 2007

Signature:

Name: Dr. Fatin A. J. Al-Moudarris

Title: (Supervisor)

Date: / 4 / 2007

Signature:

Name: Dr. Uday A. H. Al-Obaidy

Title: (Supervisor)

Date: / 4 / 2007

Approved by the University Committee of Postgraduate Studies

Signature:

Name: Dr. Laith Abdul Aziz Al-Ani

Title: (Assistant professor)

Dean of College of Science

Date: / 4 / 2007

List of Symbols

a	Aperture radius of the quadrupole lens (bore–radius) (mm).
b	The radius of spherical electrodes (mm).
$C_{30}/d, C_{12}/d$	Relative spherical aberration coefficients of the quadrupole lens in the convergence plane.
C_{cx}/d	Relative chromatic aberration coefficients of the quadrupole lens in the convergence plane.
C_{cy}/d	Relative chromatic aberration coefficients of the quadrupole lens in the divergence plane.
C_{mx}	Relative chromatic aberration coefficients of changing of magnification of the quadrupole lens in the convergence plane.
C_{my}	Relative chromatic aberration coefficients of changing of magnification of the quadrupole lens in the divergence plane.
$D_{03}/d, D_{21}/d$	Relative spherical aberration coefficients of the quadrupole lens in the divergence plane.
d	The axial extension of the field (mm).
$f(z)$	The function of the field distribution.
f_x	Focal length of the quadrupole lens in the convergence plane (mm).
f_y	Focal length of the quadrupole lens in the divergence plane (mm).

f_i, f_o	Focal points in the image and object side respectively.
K	A coefficient accounting for the shape of the electrode.
L	Effective length of lens (mm).
ℓ	Geometrical length of lens (mm).
M_y	Magnification of the quadrupole lens in the divergence plane
M_x	Magnification of the quadrupole lens in the convergence plane
r	Radial displacement of the beam from the optical axis (mm).
R_1	The radius of cylindrical convex electrodes (mm).
u	Object distance from starting point of the field of the lens (mm) .
v	Image distance from the end of the field of the lens (mm) .
V_1	Electrode voltage (volt).
V_o	Accelerating voltage (volt).
$V(r,\theta,z)$	Axial potential distribution (volt).
z	Optical axis (mm).
β	Quadrupole lens excitation parameter ($\beta^2 = V_1 K / a^2 V_o$) (mm^{-1}).
2Γ	Gap angle between the electrodes (degree).
2γ	Electrode angle (degree).

References

Abramovich, S., Zavjalov, V., Zvenigorodsky, A., Ignatev, I., Magilin, D., Melnik, K., and ponomarev, A. (2005)

Optimization of the prop-forming system a scanning nuclear microprobe based on the EGP-10 electrostatic tandem .

Tech. phys. , **50** (2),146-151

Baartman, R. (1995)

Intrinsic third order aberration in electrostatic and magnetic quadrupoles.

Trumf-DN, 95, 21

Baranova, L. A. and Read, F. H. (1998)

Reduction of the chromatic and aperture aberrations of the stigmatic quadrupole lens triplet

Optik, **109**(1), 15–21

Baranova, L. A. and Read, F. H. (1999)

Minimisation of the aberrations of electrostatic lens systems composed of quadruple and octupole lenses.

Int. J. Mass Spectrum, **189**, 19–26

Baranova, L. A. and Read, F. H. (2001)

Aberration caused by mechanical misalignment in electrostatic quadrupole lens systems

Optik, **112** (3), 131–138

Baranova, L. A. , Ovsyannikova, L. , and Yavor, S. Ya. (1972)

Asymmetric quadrupole lenses.

Sov.Phys.Tech.Phys., **17** (1), 170-172

Baranova, L. A. , Yavor, S.Ya., and Read, F.H. (1996)

Crossed aperture lenses for the correction of chromatic and aperture aberrations.

Rev. Sci. Instrum., **67**, 756–760

Baranova, L. A. and Yavor, S.Ya. (1984)

Electrostatic lenses.

Sov.Phys.Tech.Phys., **29** (8), 827-847

Barnes, H., Schilling, D., David, M., Koppenaal, W., Hieftje ,M. (2003)

Development and characterization of an electrostatic quadrupole extraction lens for mass spectrometry.

Int. J. Mass Spectrum, **18**, 1015–1018

Bosi, G. (1974)

Quadrupole fields in circular concave electrodes and poles

Rev. Sci. Instrum., **45**(10), 1260–1262

Cosslett, V.E. (1950)

Introduction to electron optics.

Second Edition, (Oxford, Clarendon)

Dymnikov, A. D., Brenner, J. (2000)

Theoretical study of short electrostatic lens for the Columbia ion microprobe .

Rev. Sci. Instrum., **17** (4), 1646-1650

Dymnikov, A. D., Fishkova, T. Ya., and Yavor, S. Ya. (1965)

Spherical aberration of compound quadrupole lenses and systems

Nucl. Instrum. Meth., **37**, 268–275

Dymnikov, A. D., Glass, G.A., and Rout, B. (2005)

Zoom quadrupole focusing systems producing an image of an object

Nucl. Instrum. Meth. Phys. **B241**, 402–408

Fishkova, T. Ya., Baranova, L. A., and Yavor, S. Ya. (1968)

Spherical aberration of stigmatic doublet of quadrupole lenses (rectangular model).

Sov.Phys.Tech.Phys., **13** (4), 520-525

Fishkova, T. Ya., and Yavor, S. Ya. (1968)

Correction of the spherical aberration of quadrupole lenses by means of octupoles.

Sov.Phys.Tech.Phys., **13** (4), 514-518

Geriach, R. L., Utlaut M. W. (2001)

Angular aperture shaped beam system and method .

United State Patent ,6977386(09/765)

Gillespie, G. H. (2005)

Optics elements for modeling electrostatic lenses and accelerator components IV.
Electrostatic quadrupoles.

Nucl. Instrum. Meth. Phys. , **A 427** (1), 315–320

Grime, G.W., and Watt, F. (1988)

Focusing proton and light ions to micron and submicron dimensions

Nucl. Instrum. Meth., **B30**, 227–234

Grivet, P. (1972)

Electron Optics

(*Pergamon Press, Oxford and New York*)

Guharay, S. K., Allen, C. K., Yang, V. (2001)

Low energy H^{-} beam transport using an electrostatic quadrupole focusing system .

Rev. Sci. Instrum., **56** (5), 1774-1777

Hawkes, P.W. (1965/1966)

The electron optics of a quadrupole lens with triangular potential

Optik, **23**, 145–168

Hawkes, P.W. (1967)

Real and virtual quadrupole aberrations.

Optik, **25**, 315–320

Hawkes, P.W. (1970)

Quadrupoles in electron lens design

Adv. Electronics and Electron Phys., *Supplement 7*, ed. Marton, L.

(*Academic Press, New York and London*)

Hawkes, P.W. (1973)

Image processing and computer-aided design in electron optical.

(*Academic Press, London*)

Hayashi, T., and sakudo N. (1968)

Quadrupole field in circular concave electrodes .

Rev. Sci. Instrum., **39** (7), 958-961

Jamieson, D. N. and Legge, G. J. (1988)

Multipole lenses and their application in nucroprobe lens systems.

Nucl. Instrum. Meth. Phys. , **B30**, 235–241

Katsumi, U. (1991)

New normalization in optical properties of the electrostatic quadrupole lens

J. Elect. Micro. **40**,(6), 374-377

Kiss, A. and Koltay, E. (1970)

Investigations on the effective length of asymmetrized quadrupole lenses .

Nucl. Instrum. Meth. **78**, 238–244

Larson, J. D. (1981)

Electrostatic ion optics and beam transport for ion implantation

Nucl. Instrum. Meth., **189**, 71–91

Martin, F. W., and Goloski, R. (1981)

An achromatic quadrupole lens doublet for positive ions.

Appl. Phys. Lett., **40**(2), 191-193

Martin, F. W. (1991)

Optical parameters of MeV ion microprobes

Nucl. Instrum. Meth., **B54**, 17–23

Matsuda, H., and Wollnik, H. (1972)

Third order transfer matrices for the fringing field of magnetic electrostatic quadrupole lenses .

Nucl. Instrum. Meth., **103**, 117–124

Markovich, M. G. (1972)

Short quadrupole ,hexapole ,and octupole lenses as aberration correctors for electyron-beam deflection .

Sov.Phys.Tech.Phys.,**17** (1)

Nakata S. (1993)

A new concave electrostatic lens with periodic electrode configuration.

Rev. Sci. Instrum., **64** (6), 1432-1436

Novgorodtsev, A. B. (1982)

Quadrupole condensing lenses with a highly linear electric field distribution

Sov.Phys.Tech.Phys.,**27** (10), 1257-1260

Okayama, S. (1989)

Electron beam lithography using a new quadrupole triplet

SPIE, Electron-beam, X-ray, and Ion-beam Technology: Submicrometer Lithographies VIII, **1089**, pp 74–83

Okayama, S. and Kawakatsu, H. (1978)

Potential distribution and focal properties of electrostatic quadrupole lenses

J. Phys. E: Sci. Instrum., **11**, 211–216

Okayama, S. and Kawakatsu, H. (1982)

A new correction lens.

J. Phys. E: Sci. Instrum., **15**, 580–586

Ovsyannikova, L. P., and Yavor, S. Ya. (1969)

Third-order of asymmetrized quadrupole lenses.

Nucl. Instrum. Meth., **74**, 185–190

Regenstreif, E. (1967)

Focusing with quadrupole, doublet, and triplets

Focusing of Charged Particles, ed. A., Septier, pp 353–410

(*Academic Press, New York*)

Rose, H., Wan, W. (2005)

Aberration correction in electron microscopy.

IEEE, Proceeding of 2005 Particle Conference, Knoxville, Tennessee

Sakudo, N. and Hayashi, T. (1975)

Quadrupole electrodes with flat faces.

Rev. Sci. Instrum., **46**, 1060-1062

Schott, W. and Springer, K. (1973)

Calculations and measurements for a magnetic quadrupole lens with a large aperture and a bell -shaped field distribution.

Nucl. Instrum. Meth., **111**, 541–547

Shimizu, H., Currell, J., Ohtani, S., Sokell, E., Ymada, C., Hirayama, T., and Sakurai, M. (2000)

Characteristics of the beam line at the Tokyo electron beam ion trap.

Rev. Sci. Instrum., **71** (2), 681-683

Strashkevich, A. M. (1963)

Spherical aberration of quadrupole electrostatic lenses.

Sov.Phys.Tech.Phys., **8** (5), 380-384

Szabo` G. Y. (1975)

Geometrical aberration of the combination of asymmetrically fed quadrupole lenses and magnetic sector.

Nucl. Instrum. Meth., **125**, 339–343

Szabo` G. Y. and Ovsyannikova, L. P. (1971)

Aberrations of asymmetricized quadrupole lenses.

Nucl. Instrum. Meth., **91**, 407–411

Szilagyi, M. (1976)

Electrostatic multipole lenses with cylindrical concave electrodes.

Optik, **46**(2), 211-218

Szilagyi, M. (1988)

Electron and ion optics

(*Plenum Press, New York*)

Welsch, P., Grieser M., and Ullrich, J. (2004)

An electrostatic quadrupole doublet with an integrated steer.

IEEE, Proceeding of EPAC 2004, Lucerne, Switzerland.

Yamazaki, Y., Nagano, O., Hashimoto, S., Ando, A., Sugihara, K., Miyoshi, M., Okumura, K. (2002)

Electron optics using multipole lenses for a low energy electron beam direct writing system.

J.Vac. Sci. Tech., **B20**, (1), 25 - 30

Republic of Iraq
Ministry of Higher Education and Scientific Research
Al-Nahrain University
College of Science
Department of Physics



Determination Of The Most Favorable Shapes For The Electrostatic Quadrupole Lens

A Thesis

Submitted to the College of Science at
Al-Nahrain University in Partial Fulfillment of the
Requirements for the Degree of
Master of Science
in Physics

by

Sura Allawi Obaid Al-Zubaidy

(B.Sc. 2004)

in

Moharam 1428 A. H.

February 2007 A. D.

سورة الرعد

(فَأَمَّا الزَّبَدُ فَيَذْهَبُ جُفَاءً وَأَمَّا
مَا يَنْفَعُ النَّاسَ فَيَمْكُثُ فِيهَا
الْأَرْضِ)

صدق العظيم

من الآية (١٧)
سورة الرعد

الخلاصه

في هذا البحث أجريت حسابات توزيع المجال المحوري والخواص البصرية للعدسة الكهروسكونيه رباعية الأقطاب باستخدام طريقة المصفوفات الأنتقاليه التي أخذت أشكال أقطاب وتهيج مختلفة مثل؛ الأقطاب الأسطوانية المحدبة والكرويه. حُسب مسار حزمه الجسيمات المشحونه التي تقطع أنموذج الجهد بحل معادلة المسار للحركه في الأحداثيات الكارتيديه. حُسبت الخواص البصرية للعدسة الكهروسكونيه رباعية الأقطاب بمساعدة مسار الحزمة على طول محور العدسه. بالإضافة إلى ذلك أجريت حسابات الأمثليه لإيجاد أفضل خواص بصرية وتصميم لشكل القطب للعدسة الرباعية.

الحسابات ركزت بشكل رئيسي على حساب معاملات اشكال القطب والتهيج و الأبعاد البؤرية والتكبير ومعاملات الزيغ لكلا المستويين العمودي والأفقي للمسار على امتداد المحور البصري لكل تصميم. جرى إيجاد أمثل قيم لمعاملات الزيغ الكروي واللوني عن طريق تغير الأشكال الهندسيه للأقطاب مع الأخذ بنظر الاعتبار زوايا بينيه مختلفه للقطب.

توضح النتائج ان اختيار مدى محدد من الأبعاد الهندسيه مثل الزاويه البينيه او نسبة نصف قطر القطب الى نصف قطر الفتحة تعطينا الخواص الأمثل والأفضل لقيم معاملات الزيغ.



جمهورية العراق
وزارة التعليم العالي والبحث العلمي
جامعة النهرين
كلية العلوم
قسم الفيزياء

حساب افضل الاشكال للأقطاب لعدسه كهروسكونيه رباعية الأقطاب

رسالة

مقدمه الى كلية العلوم في جامعة النهرين

وهي جزء من متطلبات نيل درجة

ماجستير علوم في

الفيزياء

من قبل

سرى علاوي عميد الزبيدي

بكالوريوس ٢٠٠٤

في

شباط ٢٠٠٧م

محرم ١٤٢٨هـ

A decorative border with a repeating geometric pattern of diamonds and circles, framing the entire page.

Dedicated To

My Parents And

Brothers And Sisters

CHAPTER
ONE
INTRODUCTION

CHAPTER

TWO

THEORETICAL CONSIDERATION

CHAPTER
THREE
RESULTS AND DISCUSSION

CHAPTER
FOUR
CONCLUSIONS AND
RECOMMENDATIONS FOR
FUTURE WORK

